NASA CONTRACTOR REPORT

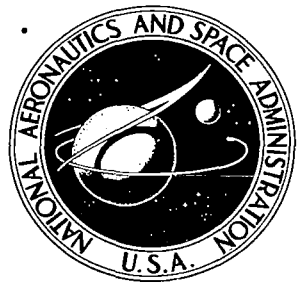

NASA CR-1118

NASA CR-1120

STUDY OF NEW METHODS TO MEASURE LOW PRESSURE

by Richard Hecht

Prepared by
NATIONAL RESEARCH CORPORATION
Cambridge, Mass.
for Langley Research Center

NATIONAL AERONAUTICS AND SPACE ADMINISTRATION • WASHINGTON, D. C. • AUGUST 1968

STUDY OF NEW METHODS TO MEASURE LOW PRESSURE

By Richard Hecht

Prepared under Contract No. NAS 1-5347, Task 3 by
NATIONAL RESEARCH CORPORATION
Cambridge, Mass.

for Langley Research Center

NATIONAL AERONAUTICS AND SPACE ADMINISTRATION

For sale by the Clearinghouse for Federal Scientific and Technical Information
Springfield, Virginia 22151 – CFSTI price $3.00

TABLE OF CONTENTS

STUDY OF NEW METHODS TO MEASURE LOW PRESSURE

By Richard Hecht
Norton Exploratory Research Division
National Research Corporation

SUMMARY

The objective of this program (NAS1-5347, Task 3) as originally defined, was the discovery of new methods for the measurement of gas pressure or density, through a systematic review of the physical properties of gases at low pressures. In the course of this study, a particularly promising area for investigation presented itself, namely, the improvement in sensitivity of absolute pressure measurements. In the present state-of-the-art, even modest improvements in absolute pressure measurement would lead to much greater accuracy in the calibration of low-pressure instruments such as ionization gauges. Accordingly, we requested and received authorization to concentrate our efforts on a theoretical and experimental evaluation of the performance of absolute pressure sensors. This final report presents the results so obtained. This is the Summary Technical Report covering the work performed by National Research Corporation under Contract NAS1-5347,Task 3 during the period November 10, 1965 to November 30, 1966.

STUDY OF NEW METHODS TO MEASURE LOW PRESSURE

By Richard Hecht

INTRODUCTION

If the outcome of a measurement will be the same for all ideal gases at the same pressure, and if the pressure can be inferred directly or indirectly from the measurement, the measurement is said to be an absolute pressure measurement. This definition, of course, includes the direct measurement of force per unit area, say by the observations of the deflections of a mercury column or an elastic membrane. However, the McLeod gauge is also an absolute pressure gauge, although it actually measures compressibility, since all ideal gases maintain the same fixed relation between pressure and compressibility. The Knudsen gauge, which measures momentum transport between surfaces of unequal temperature, is an absolute pressure gauge when operated under conditions where inter-molecular collisions are negligibly infrequent, and where full thermal accomodation of molecules at the surfaces may be assumed. On the other hand, measurements made with ionization gauges, friction gauges, and the thermocouple gauges are not absolute, since their outcome depends strongly on gas composition. If non-absolute gauges are to be calibrated, the primary standard should clearly be an absolute gauge. It must be realized, however, that the overlap range between typical ionization gauges and the standard McLeod gauge is quite meager, and since the ionization gauges are non-linear in this overlap range, the extrapolation of such calibration is uncertain. It is,

therefore, of great practical importance to seek to extend the range of absolute pressure measurement; it is hoped that the gauges to be discussed will operate reliably at pressures of 10^{-6} Torr and below.

Even though a pressure measurement may be absolute, its outcome must still be interpreted with regard to the actual experimental conditions. For example, the directly measured force per unit area, expressed in dynes/cm^2, can be converted to internal gas pressure, expressed in Torr, through the relation 1 Torr = 1.33 x 10^3 dynes/cm^2, provided that the gas is in thermodynamic equilibrium with respect to the sensing surface. By this we mean that the gas leaving the sensing surface has the same density and velocity distribution as the arriving gas, a condition which is ordinarily satisfied in static measurements. However, if the gas should have some net mass motion with respect to the sensing surface, or should have a different temperature than the sensing surface, or if there should be a net adsorption or desorption of gas at the surface, corrections will be necessary in order to infer the true internal gas pressure.

We will, however, not be concerned with the corrections of this sort in discussing, in the following section, the physical limitations of absolute pressure measurements. Rather, we will seek to establish expressions for the minimum detectable pressure under ideal conditions and, in subsequent sections, to discuss experimental arrangements which might be expected to approach these limits. The topics to be considered are the direct measurement of static pressure, the measurement of momentum transport, and the measurement of energy transport. One of these,

static pressure measurement, has been the subject of a theoretical and experimental study in depth. In this study, a gauge has been developed which will be referred to as an "electrostatically-tuned capacitance-manometer". A description of the gauge will take up the bulk of this report. Less consideration has been given to momentum transport measurements and to energy transport measurements, but possibilities for two other gauges will be discussed. These will be referred to as the "superconducting-bolometer gauge" and the "modulated gas-temperature gauge". Finally, recommendations for further study will be made.

LIST OF SYMBOLS

a:	diaphragm radius
A:	area of mechanical sensor
c:	velocity of light
C:	differential-capacitance, also, heat capacity
d:	electrode-diaphragm separation
f:	frequency
J:	current density
J_o:	zeroth order Bessel function of first kind
J_1:	first order Bessel function of first kind
k:	Boltzmann's constant, also, a wave-number of the vibrating diaphragm ($k^2 = \mu\omega^2/T$)
k_o:	a wave-number of the vibrating diaphragm ($k_o^2 = \mu\omega_o^2/T$)
k_v:	a wave-number of the vibrating diaphragm ($k_v^2 = V^2/2\pi d^3 T$)
K:	mechanical stiffness of sensor, also, thermal conductivity
L:	length
M:	sensor mass, also, molecular weight
p:	pressure
P:	pressure
P_{rad}:	pressure at which molecular and radiant energy fluxes are equal
P'_{rad}:	pressure at which molecular and radiant momentum fluxes are equal
P_n:	noise power
P_ϕ:	pressure error arising from uncertainty in work function
q, q_o:	heat flux

Q:	thermoelectric power
Q_τ:	energy flux from source whose temperature is modulated with amplitude τ
Q_v:	energy flux from source whose velocity is modulated with amplitude v
r:	radial coordinate
R:	ratio of static voltages applied to the two electrodes, also, electrical resistance
R_τ:	momentum flux from source whose temperature is modulated with amplitude τ
R_v:	momentum flux from source whose velocity is modulated with amplitude v
R_{cond}:	thermal resistance associated with conduction to heat sink
R_{gas}:	thermal resistance associated with evaporation
R_{rad}:	thermal resistance associated with radiation
S(V):	capacitance manometer output as a function of electrode voltage V
T:	absolute temperature, also, diaphragm tension
T_o:	absolute temperature of heat sink
T_s:	absolute temperature of source
v:	source velocity
V:	static voltage applied to capacitance manometer electrodes
x:	displacement of mechanical sensor
$y, y_o, y_{1...n}$:	components of diaphragm displacement
α:	error (in pressure) due to unequal spacing of capacitance manometer electrodes
β:	lumped constant in concave electrode problem
ϵ:	emissivity
ϵ_o:	bolometer emissivity
ϵ_s:	source emissivity
μ:	mass per unit area

ρ:	mass per unit volume
σ:	Stefan-Boltzmann constant
$\sigma(V)$:	capacitance manometer sensitivity as a function of electrode voltage V
τ:	amplitude of temperature modulation
ϕ:	work function
ω:	angular frequency

LOWER LIMITS OF ABSOLUTE PRESSURE MEASUREMENT

Direct Pressure Measurement

We are concerned here with measuring the displacement of a solid sensor in response to a pressure differential across the sensor. The sensor might be a piston, a diaphragm with sealed edges, a freely suspended flap between two chambers, etc. For the purposes of discussion, we shall assume that the sensor can be characterized by a mass M, an area A and a mechanical stiffness K, although these quantities may not, in actuality, be sharply defined. We will further suppose that there is a perfect vacuum behind the sensor, so that PA = Ky, where P is the pressure to be measured, and y is the displacement.

We note first that random thermal motion of the sensor imposes a theoretical lower limit on the detectable displacement, and hence on the detectable pressure. According to the thermodynamic principle of equipartition of energy, the mean-square value of the random displacement is given by $\overline{y^2} = kT/K$. Since the fundamental frequency of oscillation for the sensor is given by $\omega^2 = K/M$, we may express the thermal-noise limit for pressure detection, in cgs units, as

$$P_{noise} = \frac{\omega}{A}\sqrt{MkT} \quad \text{dynes/cm}^2 \qquad (1)$$

Of course, we can only hope to measure pressures approaching this limit if the corresponding displacements are observable in practice. As an illustration, let us consider a typical mechanical manometer, incorporating a

titanium diaphragm 5cm in diameter, .001 cm thick, and under a tension of 5×10^5 dynes/cm, so that the fundamental resonant frequency will be about 2000 cps.* Under pressure, the displacement of the diaphragm will be about 4×10^{-3} cm/Torr.*

At room temperature, thermal noise will limit the detectable pressure to about 4×10^{-8} Torr. However, for this instrument, the thermal noise limit is irrelevant, since the corresponding displacement of 6×10^{-10} cm is unobservably small; as a practical matter, displacements of less than 10^{-6} cm are quite difficult to measure.

Clearly, if an instrument is totally insensitive to thermal noise, one might surely hope to improve both its sensitivity and its signal-to-noise ratio. Suppose that we fix the mass M, the area A, and the minimum detectable displacement x_{min} of a static pressure sensor, then $P_{min} = \mu\omega^2 x_{min}$, where $\mu = M/A$, and where $\omega^2 = K/M$. Now P_{min} decreases as ω^2, while P_{noise} decreases as ω. Therefore, it will always be possible in principle to reach the thermal noise limit by reducing the resonant frequency of the sensor sufficiently. The crux of the matter is that if static pressures are to be measured, one simply has no need of a broad-band pressure sensor, and since bandwidth has been introduced at the cost of sensitivity, one should seek to reduce the resonant frequency of the instrument. Now there are practical limitations on the maximum area, minimum weight and minimum detectable displacement for static pressure sensors, so that if the theoretical noise limit of detectable pressure is to be approached, one must seek to reduce the stiffness K.

As an example, let us consider a static pressure sensor for which M = .1 gm, A = $10 cm^2$, and x_{min} = 100 Å. By reducing K to about 5×10^{-2} dynes/cm^2, we find that at room temperature, P_{noise}

---

* For a circular membrane of radius a, tension T, and mass/unit area μ, the fundamental resonant frequency f is given by $2\pi af = 2.405\ T/\mu$. Under pressure P, the displacement y at a radical distance r is given by $y = P(a^2-r^2)/4T$.

$P_{min} \approx 3 \times 10^{-12}$ Torr. The period of vibration for the sensor will then be about 10 sec. Such a sensor might consist of a flap suspended by a very light torsion fibre, similar to that employed in the Knudsen gauge. Its theoretical sensitivity would be higher than that of the Knudsen gauge because it would not be limited by radiation pressure background, but it would presumably suffer the same disadvantages of delicacy and sensitivity to vibrations. For absolute pressure measurements over a more modest range, say 10^{-2} Torr to 10^{-6} Torr, it would be preferable to improve the inherently simple and sturdy diaphragm gauge as follows:

Consider a metal diaphragm whose rest position is midway between a pair of electrodes. If a common voltage is applied to the electrodes, the electrostatic energy of the diaphragm will be a maximum at the rest position, while the elastic energy will be a minimum. Hence, the applied voltage reduces the energy gradient in the neighborhood of the rest position, i.e., reduces the available restoring force on the diaphragm. If pressure is applied to one side of the diaphragm, the diaphragm will move further, but more sluggishly, than in the absence of voltage. Thus the sensitivity of the diaphragm is increased, very much as if the tension in the diaphragm had been reduced. However, the restoring force on the diaphragm is here provided by the difference between two energy gradients, each of which will have inevitable uncertainties, so that the relative uncertainty in sensitivity will increase in direct proportion to the sensitivity itself. To avoid this self-defeating process, it will be necessary to monitor the sensitivity. A convenient method, which does not interfere with the continuous measurement of pressure, is to induce and observe mechanical resonance of the diaphragm; it will be shown in a subsequent section that the sensitivity can be precisely inferred from the values of the mechanical resonant frequency, the dimensions of the diaphragm and the electrodes, and the mass of the diaphragm. The importance of such a result is that it

guarantees that the gauge sensitivity can be calculated from known invariant quantities, rather than from uncertain quantities such as the electrostatic fields and the diaphragm tension. Furthermore, if one chooses to calibrate the gauge at high pressure against a low-sensitivity standard such as the McLeod gauge, the gauge sensitivity can be subsequently increased by tuning it electrostatically to a lower frequency, and the original calibration will remain valid.

Energy and Momentum Transport

At pressures low enough so that gas molecules collide only with the surfaces of the vacuum system, and assuming for simplicity that there is full thermal accomodation of molecules at these surfaces, the kinetic energy of a gas molecule can depend only on the temperature and velocity of the last surface struck. Energy and momentum transport between surfaces can be then accurately controlled by modifying the surface temperatures and velocities, and this has historically provided the basis for many types of pressure gauges. Clearly, there are four general physical arrangements to be considered, viz., the measurement of energy or momentum transport between surfaces of unequal temperature, and the measurement of energy or momentum transport between surfaces of unequal velocity. We shall see that two of these, viz., energy transport between surfaces of unequal velocity, and momentum transport between surfaces of unequal temperature, are independent of gas composition, and hence provide a basis for absolute pressure measurements. In what follows, we shall consider the physical limitations of such measurements.

Temperature Modulation

The source and detector are here considered to be two parallel infinite planes. The source is maintained at a temperature $T_s + \tau \cos \omega t$, where $\tau << T_s$. There is little loss of generality in choosing this form of temperature variation, since we shall in any

case make linear approximations in the discussions below. Furthermore, ω can be taken to be zero, in which case, our discussion would be appropriate to the Knudsen gauge.

The alternating component Q_τ of energy flux from the source is given by

$$Q_\tau = \left(\frac{9P\bar{v}}{16T_s} + 4\sigma\varepsilon_s T_s^3\right) \tau \cos \omega t \qquad (2)$$

while the alternating component R_τ of momentum flux from the source is given by

$$R = \left(\frac{3P}{4T_s} + \frac{4\sigma\varepsilon_s T_s^3}{C}\right)\tau \cos \omega t \qquad (3)$$

where $\bar{v}$ is the molecular thermal velocity, $\sigma = 5.67 \times 10^{-12}$ watts/cm^2-$^oK^4$ is the Stefan-Boltzmann constant, ε_s is the source emissivity, and $c = 3 \times 10^{10}$ cm/sec is the velocity of light, and p is in dynes/cm^2.

We note first that the molecular contribution to the energy flux Q_τ is proportional to the thermal velocity $\bar{v}$, and hence is composition-dependent, whereas the momentum flux R_τ is composition-independent. Furthermore, we see that a detector sensing Q_τ will be unsuitable for pressure measurements if the radiant contribution to Q_τ should exceed the molecular contribution. The crossover pressure, P_{rad}, at which these two contributions are equal, is given by

$$P_{rad} \simeq 2 \times 10^{-11} \varepsilon_s M T_s^7 \text{ Torr} \qquad (4)$$

where M is the molecular weight in amu. On the other hand, the molecular contribution to the momentum flux R_τ equals the radiant contribution at a far lower crossover pressure, P'_{rad} given by

$$P'_{rad} \quad 10^{-17} \varepsilon_s T_s^4 \text{ Torr} \qquad (5)$$

At $300^{\circ}K$, Eq.(4) predicts $P_{rad} \approx 10^{-3}$ Torr, whereas Eq.(5) predicts $P'_{rad} \approx 10^{-9}$ Torr; these results might have been expected, being roughly the limits of sensitivity of the thermocouple gauge and Knudsen gauge respectively. Obviously, one should expect still higher sensitivities at lower temperatures, and the ultimate limit of sensitivity will depend on detector characteristics rather than the radiant background.

The measurement of momentum flux from a temperature-modulated source is thus seen to be preferable, on two counts, to the measurement of energy flux from the same source. First, the momentum flux is independent of gas composition, so that the measurement is, in principle, absolute; second, the radiant background contribution is smaller by a factor $\bar{v}/c$. We are still faced with the choice of the most appropriate operating frequency. As discussed on page 9 above, the sensitivity of mechanical detectors will certainly decrease as the frequency increases. Furthermore, it is readily shown that, for fixed source power, the alternating temperature will also decrease in amplitude as the frequency increases. Thus it would appear advantageous to choose as low an operating frequency as possible; at zero-frequency, we would simply have a Knudsen gauge. On the other hand, there are definite practical advantages to working at some low audio frequency, e.g., amplifiers are more stable, and narrow band detection can be employed. We shall consider the use of such techniques in a later section, where the feasibility of constructing a "modulated gas-temperature gauge" will be discussed.

Velocity Modulation

Again the source and detector are considered to be two parallel infinite planes, but the source is now at fixed temperature, and is moving back and forth toward the detector with velocity $v \cos \omega t$. In this case the alternating component of energy flux from the source is given by

$$Q_v = \frac{3}{8} pv \cos \omega t \tag{6}$$

whereas the alternating component of momentum flux is given by

$$R_v = \frac{1}{2} P \frac{v}{\bar{v}} \cos \omega t \tag{7}$$

In this case, it is the alternating component of the energy flux that is composition-independent. We note further that, just as one can also establish a fixed velocity difference, i.e., ω can be zero. A simple arrangement would be to attach the detector to the end of a rotating arm, with the detector-plane parallel to the axis of rotation. Better still, one might hold the arm stationary and rotate a surrounding cylindrical shell. In any case, whether the additional velocity impressed on the gas is steady or alternating, there is no radiant background to the energy or momentum flux, so that the minimum detectable pressure is determined by the detector sensitivity. We shall consider a possible experimental arrangement for detecting the energy flux from a modulated-velocity source in a later section, where the "superconducting-bolometer gauge" is discussed.

ELECTROSTATICALLY-TUNED CAPACITANCE-MANOMETER

Theoretical Sensitivity of an Electrostatically-Tuned Diaphragm

In this section, we shall evaluate the theoretical pressure sensitivity of a diaphragm which has been "softened" by the application of electrostatic fields. It will be assumed that the diaphragm displacement is detected through the change in capacitance between the diaphragm and the same electrodes which produce the field, although our conclusions would not be significantly altered if some other means of detection were to be employed. Thus, the sensitivity will be expressed as a change in capacitance with respect to a pressure difference across the diaphragm. It will be of equal importance to us to discover the relationship between the sensitivity of the softened diaphragm and its mechanical resonant frequency, since the sensitivity becomes increasingly uncertain as the diaphragm softens. To avoid such uncertainty, the sensitivity can be inferred from the resonant frequency, which in fact can be conveniently monitored without affecting the performance of the diaphragm as a pressure sensor. Specifically, the resonant frequency can be ascertained from the response of the diaphragm to a weak alternating force; at resonance, the diaphragm motion will be in phase-quadrature with the driving force. As will be seen in the discussion of the experimental arrangement, the diaphragm can actually be tuned and locked to a chosen resonant frequency, through a feedback adjustment of the electrode voltages.

Plane-Parallel Electrodes

Employing cgs units throughout, we will consider the diaphragm to be a stretched metal membrane, of tension T, and a mass per unit area μ, whose clamped edge forms a circle of radius a. The diaphragm is faced on each side by a flat electrode, also of radius a, at a distance d. A static potential V is applied to one electrode and a potential V + v cos ωt, where $v \ll V$, is applied to the other.* Then for a pressure difference P across the diaphragm, the equation of motion for the diaphragm displacement y, at the radial position r, is given by

$$\mu\frac{d^2y}{dt^2} + \rho\frac{dy}{dt} - T\left(\frac{d^2y}{dr^2} + \frac{1}{r}\frac{dy}{dr}\right) = P + \frac{V^2}{2\pi d^3}y + \frac{vV}{4\pi d^2}\cos\omega t \quad (8)$$

where we have for convenience introduced a small damping term $\rho\frac{dy}{dt}$. On separating y into static and time-varying parts, $y = y_o(r) + y_1(r)\cos\omega t + y_2(r)\sin\omega t$, we obtain for the static displacement $y_o(r)$

---

* It is highly desirable that the electrostatic fields in the two gaps be equal when the diaphragm is at its normal rest position; otherwise the rest position of the diaphragm will change with the electrode voltage. In particular, if the electrodes are at unequal distances from the diaphragm, a compensating voltage should be applied to one electrode. Such considerations are of great practical importance, but do not significantly affect the results of the calculations presented here, and will temporarily be ignored. A discussion of the limitations introduced by such effects will be presented later.

$$\left(\frac{d^2}{dr^2} + \frac{1}{r}\frac{d}{dr} + k_v^2 \right) y_o(r) = -\frac{P}{T} \tag{9a}$$

with the solution

$$y_o(r) = -\frac{P}{k_v^2 T}\left(\frac{J_o(k_v r)}{J_o(k_v a)} - 1 \right) \tag{9b}$$

where $J_o(x)$ is the lowest-order Bessel function of the first kind, and where $k_v^2 = V^2/2\pi d^3 T$. As a result of this displacement $y_o(r)$, the capacitances between the diaphragm and the two electrodes will no longer be equal; the difference δC of these capacitances, will, in the limit $y_o << d$, be given by

$$\delta C = \frac{1}{d^2}\int_o^a y_o(r) r dr = \frac{Pa^2}{k_v^2 d^2 T}\left(\frac{J_1(k_v a)}{k_v a J_o(k_v a)} - \frac{1}{2} \right) \tag{10}$$

Returning now to Eq. (8), we solve for the alternating components of displacement, $y_1(r)\cos \omega t$ and $y_2(r)\sin \omega t$, through the substitution $Y(r) = y_1(r) + iy_2(r)$, obtaining

$$\left(\frac{d^2}{dr^2} + \frac{1}{r}\frac{d}{dr} + k^2 + k_v^2 + i\beta \right) Y(r) = -\frac{vV}{4\pi d^2 T} \tag{11a}$$

with the solution

$$Y(r) = \frac{vV}{4\pi d^2 T(k^2 + k_v^2 + i\beta)}\left(\frac{J_o(r\sqrt{k^2 + k_v^2 + i\beta})}{J_o(a\sqrt{k^2 + k_v^2 + i\beta})} - 1 \right) \tag{11b}$$

where $k^2 = \frac{\mu\omega^2}{T}$

and where $\beta = \frac{\rho\omega}{T}$

We now introduce the requirement that the driving frequency, $\omega/2\pi$, should be the mechanical resonant frequency of the electrostatically softened diaphragm. This requirement is automatically fulfilled in the actual control circuit through a feedback adjustment of the electrode potential V. The resonance condition is that $y_1(r)$ should vanish, i.e., $\mathrm{Re}(Y(r)) = 0$, and by inspection of Eq. (11b), we see that this in turn requires that $\sqrt{(k^2+k_v^2)a^2}$ be one of the roots X_n of $J_o(x)$. Only the lowest root, $X_o = 2.405$, need be considered, for unless the operating voltages are grossly inappropriate to the selected driving frequency, the admixture of higher-order modes should be negligible. Thus, at resonance,

$$k_v = \sqrt{(x_o/a)^2 - k^2} = \sqrt{\mu/T}\ \sqrt{\omega_o^2 - \omega^2} \qquad (12)$$

where $\omega_o/2\pi$ is the natural resonant frequency of the unsoftened diaphragm.

On substituting the value of k_v, given by Eq. (12), into Eq. (10), we obtain an exact expression for δC in terms of P, ω, and the physical parameters of the diaphragm and electrodes. Since δC is seen to be directly proportional to P for sufficiently small displacements, we may then express the sensitivity $\frac{dC}{dP}$ as

$$\frac{dC}{dP} = \frac{a^2}{\mu d^2(\omega_o^2-\omega^2)}\left(\frac{J_1\left(x_o\sqrt{1-(\omega/\omega_o)^2}\right)}{x_o\sqrt{1-(\omega/\omega_o)^2}\,J_o\left(x_o\sqrt{1-(\omega/\omega_o)^2}\right)} - \frac{1}{2}\right) \tag{13}$$

To make sense of this complicated expression for the sensitivity, let us consider the limits obtained in the extreme cases $\omega\to\omega_o$ and $\omega\to 0$. We then find that

$$\omega^2\frac{dC}{dP} = .361\,\frac{a^2}{\mu d^2}\left(1 - .072\,\frac{\omega_o-\omega}{\omega_o} + \cdots\right), \quad \omega\to\omega_o \tag{14a}$$

$$\omega^2\frac{dC}{dP} = .346\,\frac{a^2}{\mu d^2}\left(1 + .305(\omega/\omega_o)^2 + \cdots\right), \quad \omega\to 0 \tag{14b}$$

The quantity $\omega^2\frac{dC}{dP}$ is thus seen to be fairly constant, varying by less then 5% over the entire range of frequency from $\omega=0$ to $\omega=\omega_o$. Furthermore, $\omega^2\frac{dC}{dP}$ is seen to depend in first-order only on the quantities μ, a, and d, which are quite unlikely to change appreciably during the lifetime of the gauge. As noted earlier, the importance of such a result is that it guarantees that the gauge sensitivity can be calculated from known invariant quantities, rather than from uncertain quantities such as the electrostatic fields and diaphragm tension. Furthermore, if one chooses to calibrate the gauge at high pressure against a low-sensitivity standard such as the McLeod gauge, the gauge sensitivity can be subsequently increased by tuning it electrostatically to a lower frequency, and the original calibration will remain valid.

Concave Electrodes

In the commercial diaphragm gauge used in these experiments, the electrodes have been shaped so as to permit large displacements of the diaphragm, and a correspondingly large dynamic range, while still maintaining a high electrode-diaphragm capacitance, and a correspondingly high sensitivity. Specifically, the electrodes have been hollowed so as to conform to the shape of the fully extended diaphragm, as shown in Fig. 1, with the curvature greatly exaggerated. Indeed, it can be shown that the capacitance variations will be more linear with pressure for this geometry than for plane-parallel electrodes, providing only that $r_o \geq .9a$. However, our experimental results definitely indicate that this curvature has disadvantages in our particular application, and that it will be well to specify flat electrodes in future designs.

We begin by computing the static displacement $y(r)$ of the diaphragm under a pressure P and a tension T, given that a voltage V is applied to the concave electrodes shown above. For small displacements, the appropriate equation for $y(r)$ is

$$\frac{d^2y}{dr^2} + \frac{1}{r}\frac{dy}{dr} + \frac{P}{T} = \begin{cases} \dfrac{-V^2a^6y}{2\pi T d_o^3 (a^2-r^2)^3} & ; \ 0 \leq r \leq r_o \\ 0 & ; \ r_o < r \leq a \end{cases} \tag{15}$$

Unlike its counterpart Eq. (9a), which is appropriate to flat electrodes, Eq. (15) cannot be integrated in terms of tabulated functions. It seems desirable, then, to at-

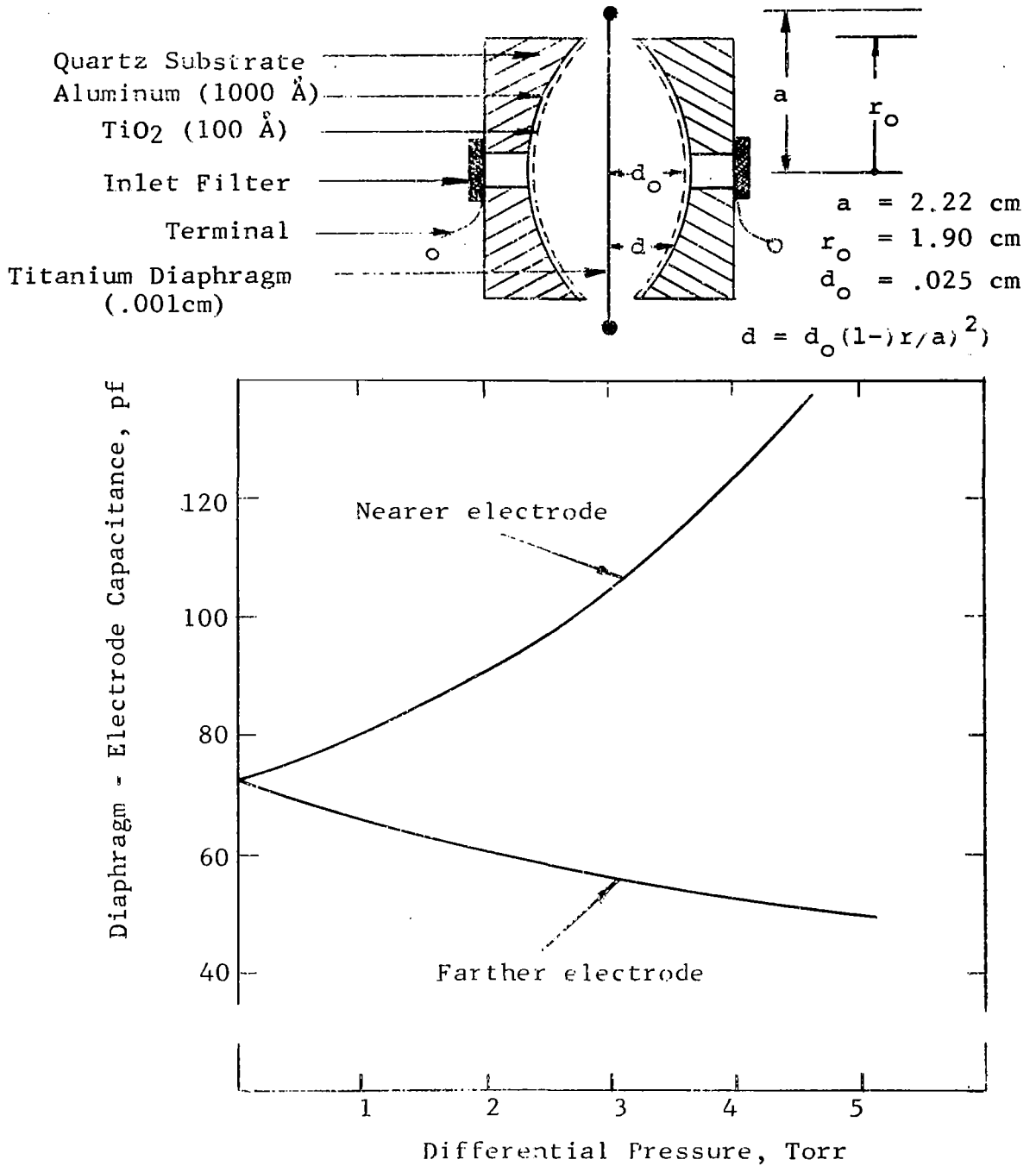

Figure 1 Commercial Diaphragm Gauge Parameters
(Lion Research 110 - CAP - 0.05D)

tempt an expansion of $y(r)$ in even powers of V. Accordingly, we set $y(r) = y_o(r) + V^2 y_1(r) + V^4 y_2(r) + \cdots$ where $y_o(r)$ is the solution of Eq. (15) for V=0, namely, $y_o(r) = P(a^2-r^2)/4T$. It follows that

$$\frac{1}{r}\frac{d}{dr}\, r\, \frac{dy_1}{dr} = \begin{cases} -\dfrac{Pa^6}{8\pi T^2 d_o^{\,3}(a^2-r^2)^2} & ; \ 0 \le r \le r_o \qquad (16a) \\ 0 & ; \ r_o < r \le a \qquad (16b) \end{cases}$$

and

$$\frac{1}{r}\frac{d}{dr} r \frac{dy_n}{dr} = \begin{cases} -\dfrac{y_{n-1} a^6}{2\pi T d_o^{\,3}(a^2-r^2)^3} & ; \ o \le r \le r_o \qquad (17a) \\ 0 & ; \ r_o < r \le a \qquad (17b) \end{cases}$$

Invoking the continuity of both y_1 and $\frac{dy_1}{dr}$ at r_o, and introducing the boundary conditions $y_1(a) = 0$ and $(dy_1/dr)_{r=0} = 0$, we obtain by direct integration of Eq. (16)

$$y_1(r) = \begin{cases} \dfrac{Pa^4}{32\pi T^2 d_o^{\,3}} \left(\ln \dfrac{a^2-r^2}{a^2-r_o^{\,2}} + \dfrac{r_o^{\,2}}{a^2-r_o^{\,2}} \ln \dfrac{a^2}{r_o^{\,2}} \right) ; 0 \le r \le r_o, \qquad (18a) \\ \dfrac{Pa^4}{32\pi T^2 d_o^{\,3}} \dfrac{r_o^{\,2}}{a^2-r_o^{\,2}} \ln \dfrac{a^2}{r^2} \qquad ; r_o < r \le a \qquad (18b) \end{cases}$$

At this point, we could substitute our solution for

$y_1(r)$ into Eq.(17) to obtain $y_2(r)$, then by successive integrations, compute $y(r)$ to any desired order in V^2. However, we can simplify matters considerably by noting that as r_o approaches a, the right-hand side of Eq.(10) will peak sharply at r_o, and that further,

$$\lim_{r \to r_o \to a} \left(\ln \frac{a^2-r^2}{a^2-r_o^2} + \frac{r_o^2}{a^2-r_o^2} \ln \frac{a^2}{r^2} \right) = \frac{r_o^2 \ln a^2/r_o^2}{(a^2-r_o^2)^2} (a^2-r^2) \qquad (19)$$

Thus we obtain, through the same integration which yielded Eq.(18), the limiting result

$$\lim_{\substack{r_o \to a \\ n=1,2,\ldots \\ 0 \le r \le r_o}} y_n(r) = \frac{P(a^2-r_o^2)}{4T} \left(\frac{a^4 r_o^2 \ln a^2/r_o^2}{8\pi T d_o^3 (a^2-r_o^2)^2} \right)^n \cdot \left(1 + \frac{a^2-r_o^2}{r_o^2 \ln a^2/r_o^2} \ln \frac{a^2-r^2}{a^2-r_o^2} \right) \qquad (20)$$

so that finally, we may express $y(r)$ as

$$\lim_{\substack{r_o \to a \\ 0 \le r \le r_o}} y(r) = \frac{P}{4T} \left(a^2-r^2 + \frac{(a^2-r_o^2)\beta V^2}{1-\beta V^2} \right) \left(1 + \frac{a^2-r_o^2}{r_o^2 \ln a^2/r_o^2} \ln \frac{a^2-r^2}{a^2-r_o^2} \right) \qquad (21)$$

where $$\beta = \frac{a^4 r_o^2 \ln a^2/r_o^2}{8\pi T d_o^3 (a^2-r_o^2)^2}$$

What is actually measured, of course, is the difference between the capacitances formed by the diaphragm and the two electrodes. For small displacements of the diaphragm, this difference is simply $\delta C = \int_o^{r_o} \frac{y(r) r dr}{d^2}$, where

$y(r)$ is given by Eq.(21). The integration is straightforward, and since $y(r)$ is linear in P, we obtain for the theoretical sensitivity

$$\frac{dC}{dP} = \frac{a^4 \ln a^2/(a^2-r_o^2)}{8Td_o^2}\left(1 + \frac{\beta V^2}{1-\beta V^2}\left(\frac{a^2-r_o^2(1-\ln a^2/r_o^2)}{a^2 \ln a^2/r_o^2 \ln a^2/a^2-r_o^2} - \frac{(a^2-r_o^2)}{a^2 r_o^2 \ln a^2/r_o^2}\right)\right) \qquad (22)$$

The quantities appearing in this expression for dC/dP are all known to within 1 or 2%, both from the manufacturer's specifications and from the measured values of total capacitance, of natural sensitivity, and of natural resonant frequency, which have all been found to be mutually consistent. On substituting these numbers into Eq.(15), we obtain for the sensitivity of the gauge employed in these experiments

$$\frac{dC}{dP} = 1.11 \times 10^{-2}\left(1 + .89\frac{(V/1260)^2}{1-(V/1260)^2}\right); \qquad \begin{array}{l} V \text{ in volts,} \\ C \text{ in Picofarads,} \\ \text{and P in microbars} \end{array} \qquad (23)$$

In order now to relate the sensitivity to the resonant frequency, we should compute the resonant frequency as a function of electrode voltage. An exact treatment would be lengthy, and for our purposes, unnecessary, since our experimental investigation has been confined to frequencies fairly close to the natural resonant frequency. We will therefore treat the applied electrostatic field as a perturbation on the freely vibrating diaphragm. The equation of motion which must be solved for ω is then

$$\frac{d^2y}{dr^2} + \frac{1}{r}\frac{dy}{dr} + \frac{\mu\omega^2}{T} = \begin{cases} \dfrac{V^2a^6}{2\pi T d_o^2 (a^2-r^2)^3}\, y & ; \ 0 \le r \le r_o \\ 0 & ; \ r_o < r \le a \end{cases} \qquad (24)$$

For small V, first-order perturbation theory gives

$$\frac{\omega_o^2-\omega^2}{\omega_o^2} = \frac{V^2a^6}{2\pi T d_o^3 k_o^2} \frac{\int_o^{r_o} J_o^2(k_o r)(a^2-r^2)^{-2} r\,dr}{\int_o^a J_o^2(k_o r) r\,dr} \approx \left(\frac{V}{1400}\right)^2 \qquad (25)$$

where ω_o is the natural resonant frequency, where $k_o^2 = \mu\omega_o^2/T$, where $y(r)$ approaches $J_o(k_o r)$ as V approaches zero, and where the parameters of the actual experimental gauge have been introduced in order to obtain the right-hand equality. As a check on this result, let us assume, by analogy with Eq.(14) obtained for flat electrodes, that the quantity $\omega^2 \frac{dC}{dP}$ is very nearly constant for the concave electrode geometry. (Intuitively, this assumption appears entirely reasonable.) Then it would be the case that the bracketed term in Eq.(23) would very nearly equal $(\omega_o/\omega)^2$, so that by comparison to Eq.(17), we would have

$$\frac{\omega_o^2-\omega^2}{\omega_o^2} = \frac{.89(V/1260)^2}{1 - .11(V/1260)^2} \qquad (26)$$

For small values of V, this result is within 3% of that given by Eq.(25). Furthermore, the observed values of resonant frequency as a function of voltage are in good agreement with both Eq.(25) and Eq.(26), although the frequency range covered is not really wide enough to provide positive confirmation for the theory. These observed values of resonant frequency, along with the theoretical values given by Eq.(25) and Eq.(26), are shown in Fig.2. As for the gauge sensitivity, Eq.(23) might well be expected to hold even

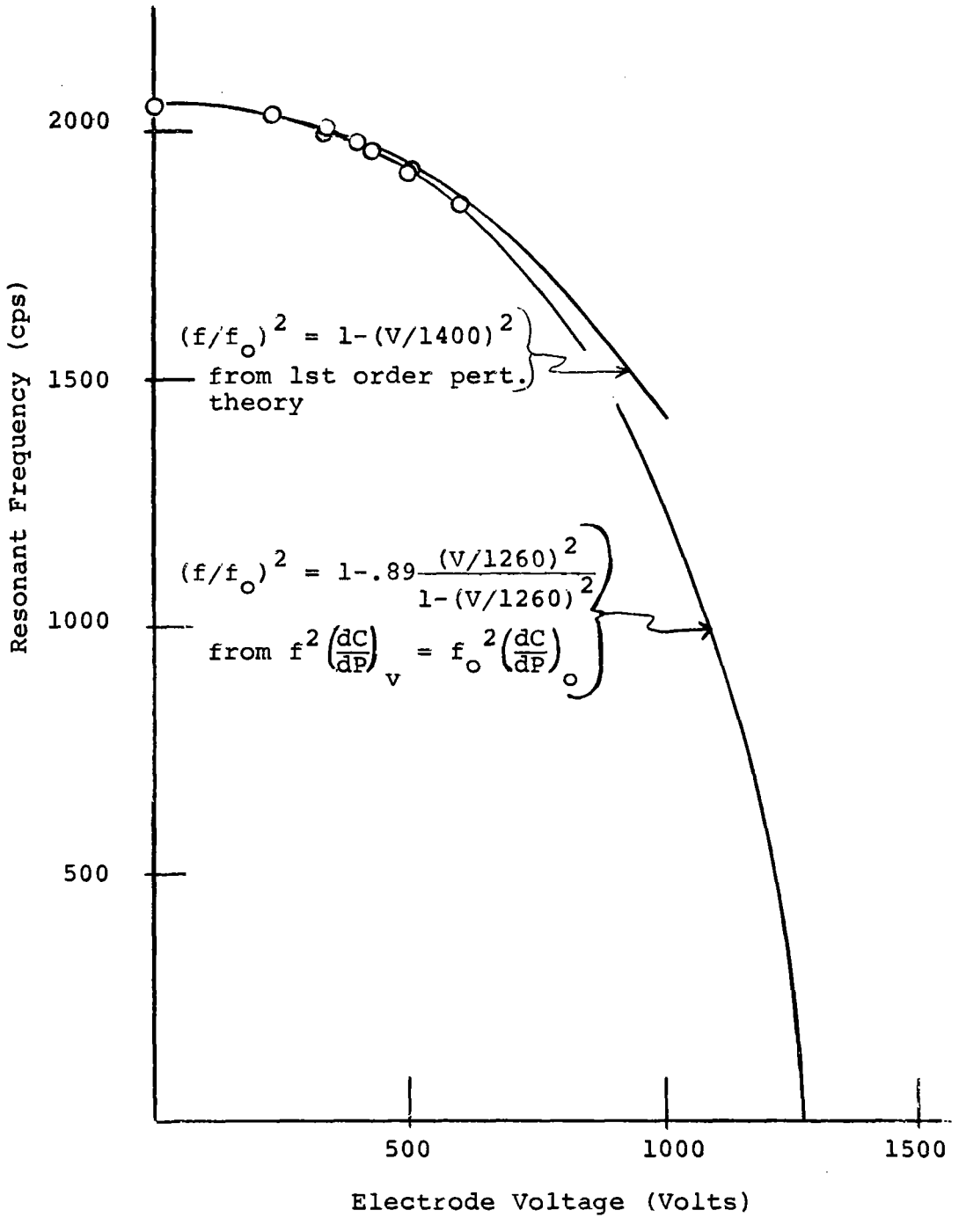

Figure 2

Resonant Frequency vs. Electrode Voltage

for values of V approaching the limiting value of 1260 volts, because the only approximation made in deriving Eq.(23) was the substitution indicated by Eq.(19); this approximation can be shown to be very nearly exact, given the actual values of r_o and a for the gauge employed in our measurements. Actually, the experimental results do not support Eq.(23) very well, but we suspect that the cause of the discrepancy is quite extraneous to the theory. We shall reserve discussion of these results until the experiment itself has been described.

Asymmetrical Electrodes

As noted earlier in this report, any lack of symmetry in the placement of the two electrodes with respect to the diaphragm will lead to an unbalanced electrostatic force on the diaphragm, and a consequent voltage-dependent shift in the rest position of the diaphragm. Now as we shall see in the discussion of the experimental arrangement, the diaphragm can readily be restored to its original rest position by applying unequal static voltages to the electrodes. The question to which we address ourselves here is simply this: For what class of asymmetries will a single ratio of electrode voltages suffice to present zero-shifts at all voltages? If the asymmetries could be restricted to this class alone, the problem of correcting zero-shifts will be far simpler than in the more general case, where the required voltage ratio will vary with voltage. The desired class of asymmetries may be found as follows:

Let $d_1(r)$ and $d_2(r)$ be the separations between the diaphragm and the two electrodes respectively, in the absence of applied voltage or pressure. We seek to discover what restrictions on $d_1(r)$ and $d_2(r)$ must exist in order that a single voltage ratio, $R=V_1/V_2$, will ensure that there will be no voltage-induced zero-shift, i.e. that in the absence of pressure, the capacitance difference $\delta C=C_1-C_2$ will be independent of voltage. This condition on δC may be expressed by the relation:

$$\int_o^a \left(\frac{1}{d_1^2(r)} - \frac{1}{d_2^2(r)}\right) y_v(r)\, r\,dr = 0 \qquad (27)$$

where the displacement $y_v(r)$ is the solution to the equation.

$$\left(\frac{d^2}{dr^2} + \frac{1}{r}\frac{d}{dr}\right) y_v(r) = \frac{V_2^2}{2\pi T}\left(\frac{R^2}{(d_1^2 - y_v)^2} - \frac{1}{(d_2 - y_v)^2}\right) \qquad (28)$$

By inspection, Eq. (27) can be satisfied for all values of V only if y_v has the functional form $y_v(r) = f(V)g(r)$. It then follows that Eq. (28) can be satisfied only if the bracketed term on the right vanishes for all V and r. It can then be seen that a single voltage ratio, $R = V_1/V_2$, will suffice to prevent zero-shifts only if $d_1(r) = Rd_2(r)$, in which case the displacement $y_v(r)$ will vanish identically. Put another way, voltage-induced zero-shifts can only be avoided if the electrostatic forces, exerted on the diaphragm by the two electrodes, cancel one another at every point on the diaphragm. Now if the electrodes have been machined to exactly equal curvature, this restriction on $d_1(r)$ and $d_2(r)$ can be satisfied either if $d_1(r) = d_2(r)$, which is practically impossible to guarantee, or if the electrodes are flat and parallel to the diaphragm, in which case R is simply the ratio of their separations. Thus, the problem of minimizing voltage-induced zero-shifts is considerably simplified if flat electrodes are employed.

Electrostatically-Tuned Capacitance-Manometer Circuit

General Description

Figure 3 is a schematic of the circuit used in testing the concept, presented above, of both increasing and monitoring the sensitivity of a conventional capacitance-manometer electrostatically. The diaphragm and adjacent electrodes form two arms of a cw rf bridge; the other two arms are fixed capacitances. Static and audio voltages are applied to the electrodes through isolating rf chokes. The diaphragm is kept in continuous vibration by the audio voltage, so that rf amplitude at the electrodes is slightly modulated at the audio frequency. If a differential pressure is now established across the diaphragm, the consequent displacement will raise the peak rf amplitude on the low pressure side. Thus, the output of the rf detector will be the sum of an audio voltage, proportional in amplitude and synchronous in phase with the diaphragm vibration, and a steady voltage proportional to the pressure differential. This steady voltage is simply extracted by filtering, and then presented to a voltmeter or recorder. In addition, the rf detector output serves to control certain feedback sub-circuits. The functions of these circuits are summarized below; a detailed discussion of the entire system follows:

Phase Detector

The phase detector automatically adjusts the static voltage applied to the electrodes, so as to tune the diaphragm to mechanical resonance at a chosen audio fre-

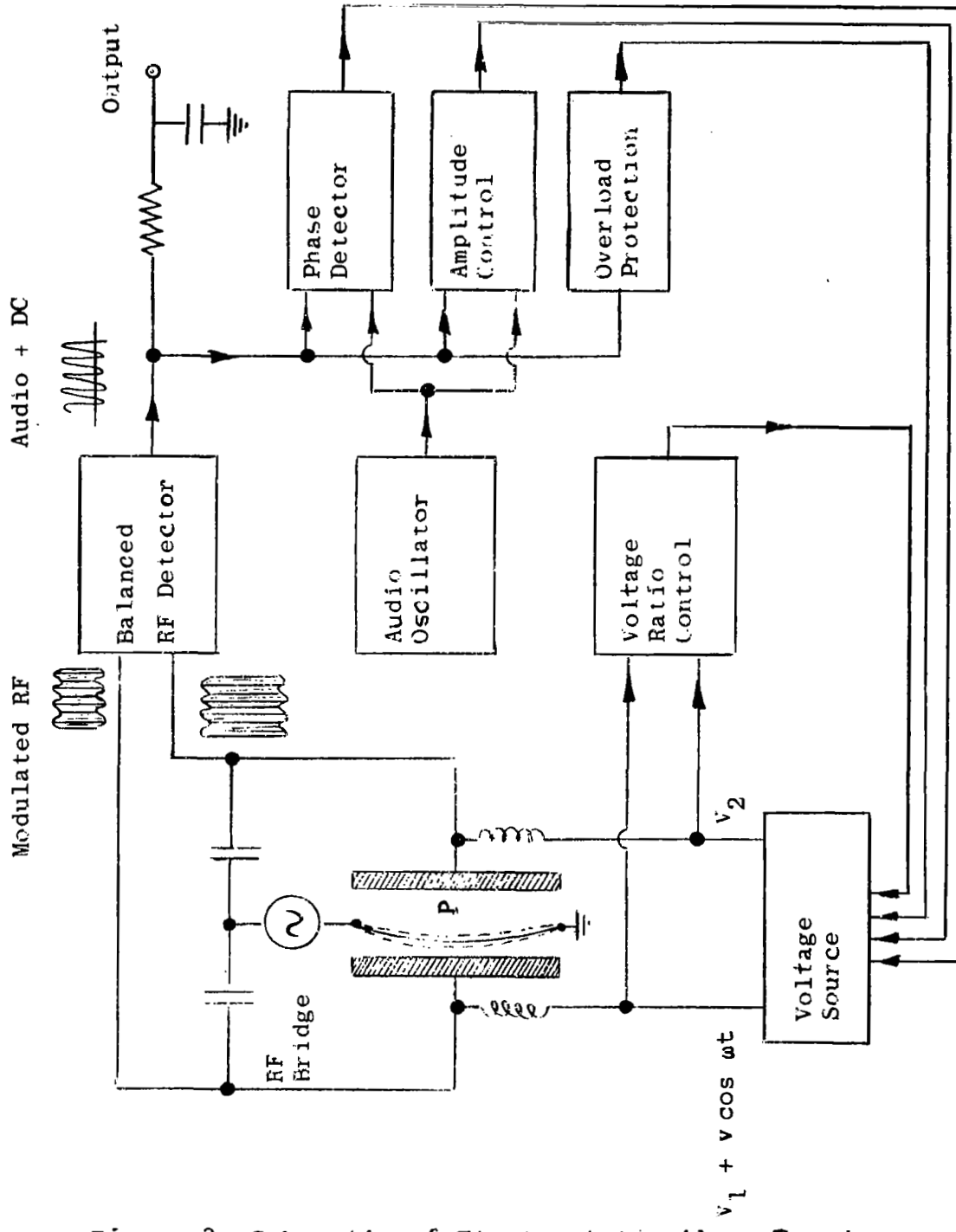

Figure 3 Schematic of Electrostatically - Tuned Capacitance-Manometer

quency. This is accomplished by a comparison of the phase of the diaphragm vibration with the phase of the electrostatic driving force; more precisely, the phase of the rf detector output is compared with the phase of a master audio-oscillator, whose amplified output produces the driving force. The resonance condition is that the phase of the diaphragm vibration should lag that of the driving force by 90°; any deviation from this condition produces an error signal which alters the static voltages so as to restore the diaphragm to resonance. Having established a chosen resonant frequency for the diaphragm, the sensitivity of the gauge may be computed from the relationships developed in the preceding section.

Amplitude Control

The amplitude control adjusts the magnitude of the electrostatic driving force so as to maintain a constant amplitude of diaphragm vibration. This simplifies the task of the phase detector described above, for if the driving force were constant in magnitude, any drift away from the resonance peak would result in a decrease in vibration amplitude, and a consequent decrease in phase detector error signal. Indeed, the resonance is only a few cycles wide, so that a small change in electrode voltage, arising say from a line-voltage fluctuation, could result in a complete loss of error signal if the driving force were not substantially increased above that required at resonance. The amplitude control is fully effective over a frequency band which extends several line-widths to either side of resonance.

Overload Protection

The overload protection circuit prevents the diaphragm from making contact with an electrode at high voltage, since this could cause pitting, or even welding, at the point of contact. The circuit is triggered when the diaphragm displacement, in either direction, exceeds some small fraction of the maximum displacement. Once triggered, the circuit first reduces the electrode voltage, thus stiffening the diaphragm, and then disconnects the high-voltage supply by means of a latching relay.

Voltage-Ratio Control

The voltage ratio control does not utilize the rf detector output, but is fed directly from the output of the high-voltage source. The function of this circuit is to maintain a fixed ratio of the static voltages at the electrodes, regardless of the magnitude of these voltages. In this way, voltage-dependent shifts in the rest position of the diaphragm can be minimized. If the static voltages applied to the electrodes were identical, such shifts would naturally arise from slight inequalities in the electrode-diaphragm separations, since the electrostatic fields on the diaphragm would not be balanced. It can be seen that if the electrodes are flat, and are parallel to the diaphragm, but are at slightly different distances from the diaphragm, a single setting of the voltage ratio will ensure that the diaphragm rest position is unaffected by voltage. For more complex irregularities, the required voltage ratio will vary somewhat with voltage, but in any case,

the shifts can be minimized. This has been discussed above in the section dealing with the effects of the electrode asymmetry.

Details of Circuit Operation

Figure 4 shows the circuit, exclusive of power supplies, in detail. The individual sections of the circuit are discussed below:

1. Capacitance Bridge

The G.R. 1330A bridge oscillator is normally operated at a frequency of about 1.5 Mc, the output amplitude being 20 volts CW. Since the bridge impedances are almost entirely capacitative, the bridge balance is fairly insensitive to the oscillator frequency. Thus, varying the oscillator frequency serves as a fine control on the balance; coarse control is provided by the ganged pair of 100 pf air-capacitors. It will be noted that there is no coupling of the static electrode voltages, and very little coupling of the audio electrode voltage, through the bridge. Thus the gains of the 6CB5 pentodes, which serve as electrode voltage sources, are not degenerated. Although the pentodes are decoupled so far as rapid variations in voltage are concerned, their independent drift, and any consequent drift in the rest position of the diaphragm, is prevented by the voltage ratio control circuit.

2. RF Detector

The rf detector circuit serves to rectify the rf voltages appearing at the electrodes, and to feed the rectified voltages to a differential amplifier (Nexus

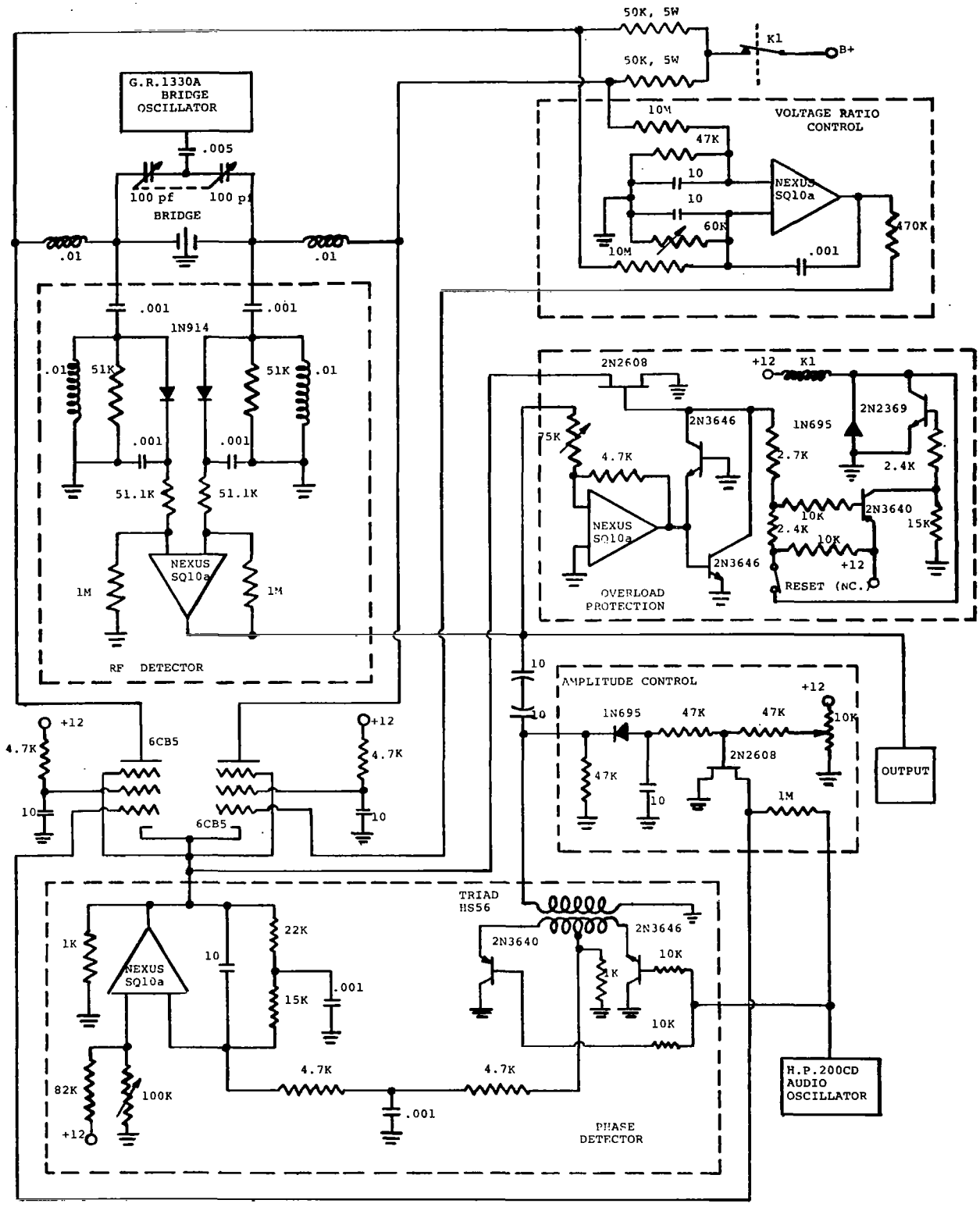

FIGURE 4 ELECTROSTATICALLY-TUNED CAPACITANCE-MANOMETER CIRCUIT

SQ10a). The .001 uf capacitors at the detector input serve to block the static electrode voltages, the .01h chokes serve to attenuate the audio electrode voltage, while the 51K resistors maintain the detector impedance independent of the bridge oscillator frequency. Matched 1N914 diodes are employed; these have been wrapped together in aluminum foil to prevent independent thermal drift. Each diode output is rf filtered by the combination of the .001 uf capacitor, the 51.1K resistor, and the 1M resistor. With this particular choice of resistors, the amplifier has a gain of 20.

The capacitance bridge, the isolating chokes connecting the electrodes to the pentode plates, and the rf detector, with the exception of the differential amplifier and 1M resistors, are all housed in a common electrostatic shield. The rf detector has been tested by substituting 100 pf fixed capacitors for the diaphragm-electrode capacitance, and the detector noise level has been found in this way to be equivalent to a change in either fixed capacitance of .001 pf. This noise level is well below that observed in actual pressure measurements, so that the shielding is certainly adequate. However, in an earlier version of this detector, we had chosen to install the diodes with opposing polarities, so that the diode outputs could be summed at one terminal of the amplifier, the other terminal being grounded. This was done to avoid the possibility of a change in amplifier gain with signal level (the common-mode effect) inherent in the present design. However, this earlier version was sensitive

to asymmetries in the rf waveform, since one diode only passed positive peaks, while the other only passed negative peaks. The present design is certainly superior, since it is the case that the common-mode rejection ratio of this amplifier is fairly high.

3. Phase Detector

The heart of the phase detector is the transistor pair, 2N3640 and 2N3646. The operation of these transistors may be understood by referring to Figure 5. An audio sine-wave of about 10 volts cw is impressed on each 10K base-resistor; the base-voltage, of course, is clipped whenever the base-collector junction is forward-biased. In the absence of base-voltage, the emitter-voltage would also be sinusoidal, with an amplitude of about 10 volts cw, as shown by the dashed line; this voltage is induced in the secondary winding of the Triad HS56 transformer by the audio output of the rf detector. However, whenever the base-emitter junction is forward-biased, the emitter will follow the base. The voltage at the secondary center-tap is then proportional to the sum of the emitter voltages, as shown in Figure 5. This description is to some extent idealized; the actual waveforms have somewhat more structure than those shown in Figure 5, partly as a result of switching transients. Be that as it may, it is clear that the average voltage appearing at the transformer center-tap will depend on the phase difference between the oscillator output and the rf detector output; this voltage serves as an error signal which brings the diaphragm to resonance, as follows:

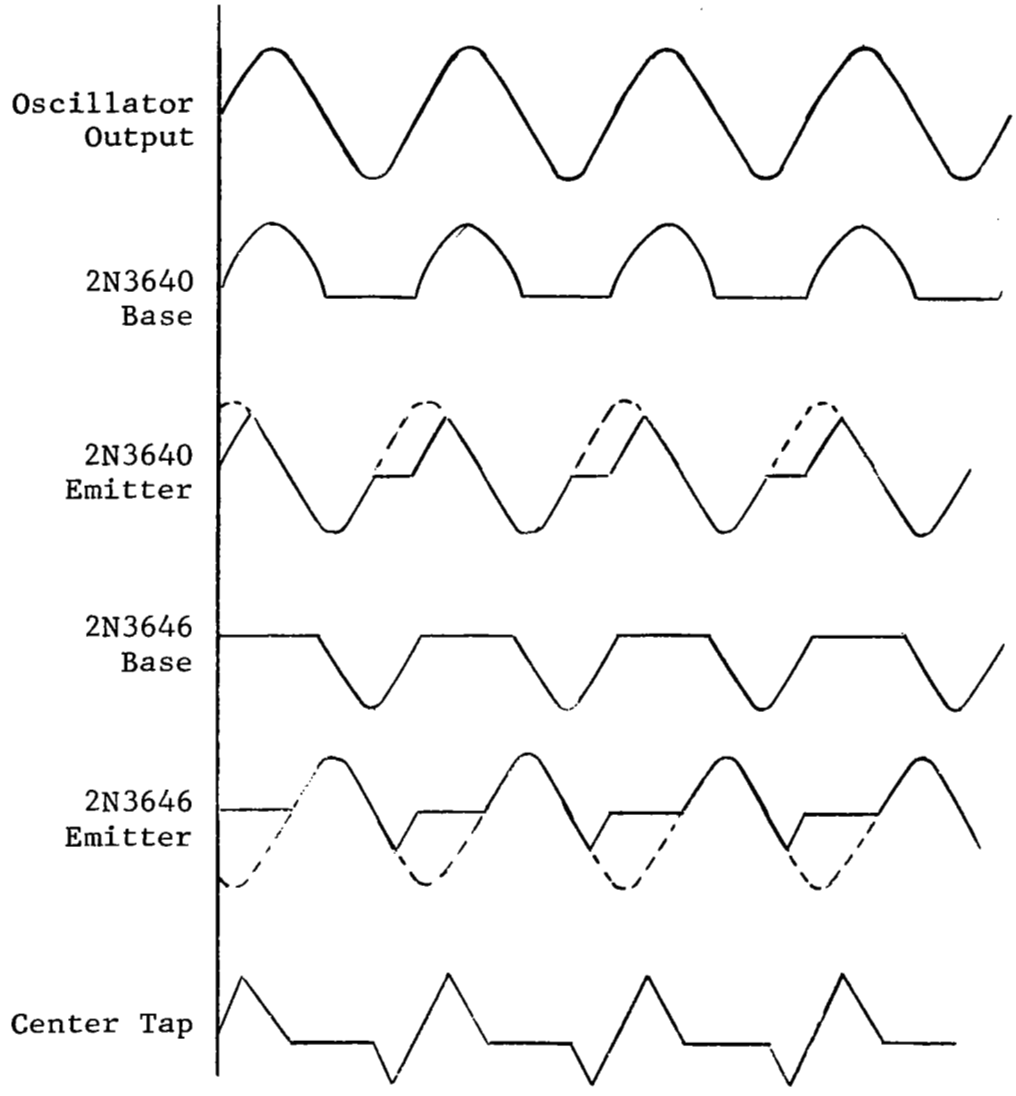

Figure 5

Waveforms of Phase Detector

The left-hand input of the Nexus SQ10a amplifier (see Figure 4) is maintained, by the voltage-divider formed by the 82K resistor and the 100K potentiometer, at a fixed positive voltage of about 1 volt. Negative feedback around the amplifier maintains the right-hand input at the same voltage. It is then clear that the continuity of current through the 37K feedback resistance and the 9.4K input resistance will establish a dc voltage gain of 4 for this amplifier. That is, the common cathode voltage of the 6CB5 pentodes will exceed the Nexus SQ10a input voltage by 4 times the voltage difference between the Nexus SQ10a input and the transformer center-tap. The capacitors in this circuit act as audio filters, while the 1K cathode resistor serves to establish a suitable quiescent current for the pentodes, about 2 ma each. Now the right-hand and left-hand control grids of the pentode pair are maintained at voltages established by the voltage-ratio control circuit and the amplitude-control circuit respectively. Thus, the error voltage, which appears at the transformer center-tap in response to a departure of the diaphragm from resonance, will in turn cause a change in the pentode plate-voltages. The feedback is entirely sufficient to restore the diaphragm to resonance, provided that the driving frequency remains within a few line widths of the resonance frequency.

Figure 6 shows observed values of plate-voltage as a function of the phase difference between the rf detector output and the audio oscillator output; these are "open-loop" values, obtained by removing the diaphragm from the circuit and then introducing a fixed-

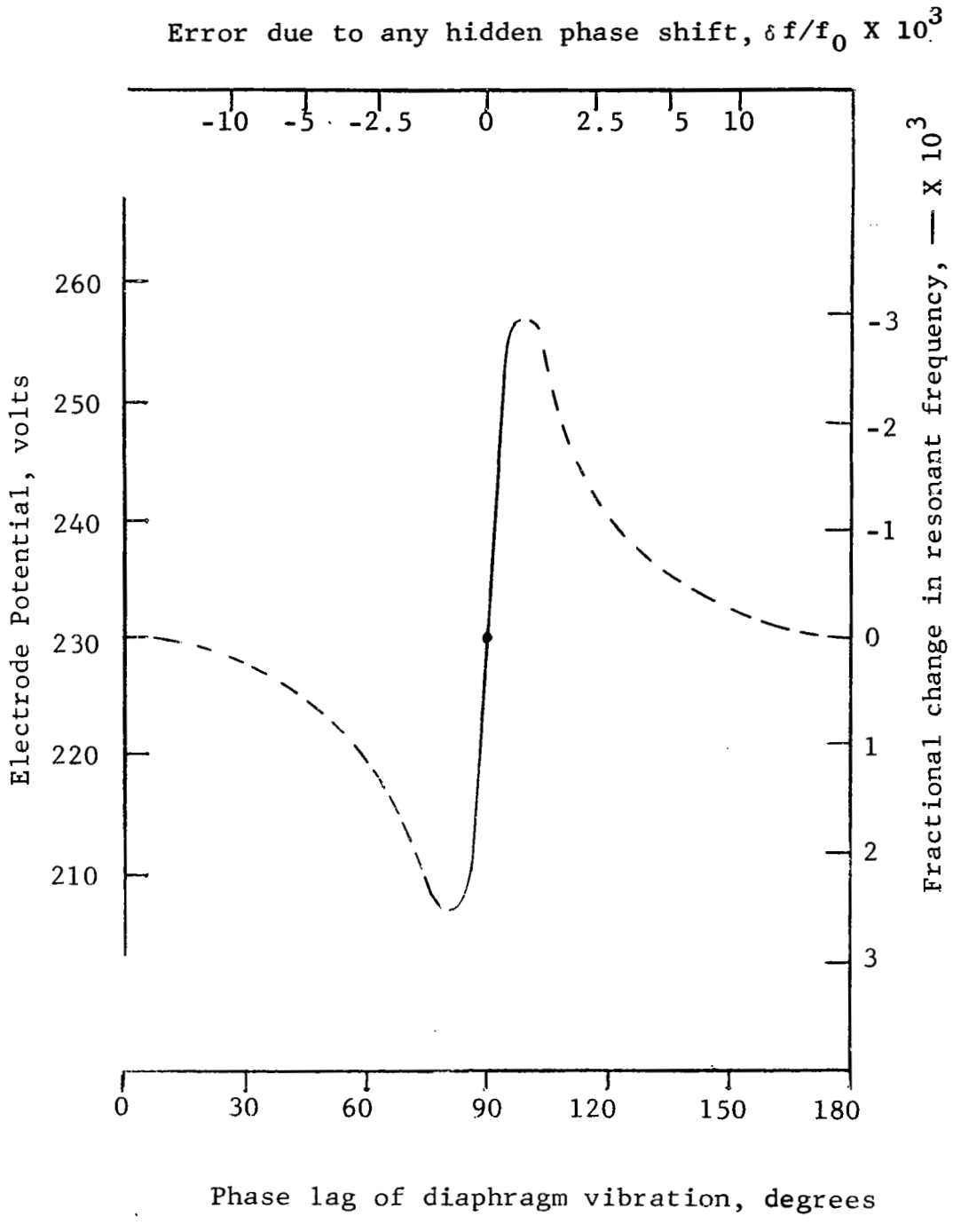

Figure 6 Characteristics of Phase Detector

amplitude, variable-phase audio voltage at the rf detector output. Figure 6 also shows estimated values of $\delta f/f_o$, the fractional difference between the driving frequency and the resonant frequency, which might arise from a hidden phase shift.* It can be seen that within the operating limits of the amplitude control circuit discussed below, the error in assuming that the driving frequency equals the resonant frequency is negligible. Indeed, in practice the resonance condition is unmistakable, provided that the pentode plate voltages are monitored; one simply increases the driving frequency from well below resonance, and notes the characteristic rise and subsequent dip in between the rise and dip.

4. Amplitude Control

An audio voltage is introduced at the left-hand control grid of the 6CB5 pentode pair (see Figure 4); the resulting audio plate voltage drives the diaphragm. This audio grid-voltage is directly obtained from a voltage divider across the HP200CD audio oscillator output, the voltage divider being formed by the 1M re-

* The displacement of a simple resonant system, such as a mass m restrained by a spring, in response to a driving force F cos ωt, is given by F sin $(\omega t+\Phi)/m\sqrt{(\omega_o^2-\omega^2)^2+(\omega\omega_o/Q)^2}$, where $\omega_o/2\pi$ is the resonance linewidth. The phase angle Φ, which vanishes at resonance, is given by $\Phi=\tan^{-1}(Q((\omega_o/\omega)-(\omega/\omega_o)))$. Now if $\omega=\omega_1-\delta\omega$, where $\delta\omega<<\omega_o$, it follows that $\Phi\simeq 2Q\delta\omega/\omega_o$. At pressures below 1 Torr, the Q of the diaphragm gauge used in these measurements is about 200. On this basis, we have arrived at the estimate of $\delta f/f_o$ shown in Fig. 6.

sistor in series with the 2N2608 FET. Thus, the amplitude of the driving voltage will vary in response to changes in the FET gate voltage. The gate voltage is established by the combined effect of a bias voltage from the 10K potentiometer and the output voltage of the 1N695 rectifier, where the latter voltage is, of course, determined by the amplitude of diaphragm vibration, as measured by the rf detector. This feedback serves to maintain a constant amplitude of diaphragm vibration, even when the driving frequency differs from the resonant frequency. The amplitude control circuit shown in Figure 4 is fully effective over a frequency band extending several line-widths to either side of resonance.

5. Overload Protection

The overload protection circuit has the function of cutting off the electrode voltages should the diaphragm move more than a few microns from its rest position; in normal operation, the amplitude of the diaphragm vibration is maintained at about 1 micron, while the static displacements are far smaller. By comparison, the full electrode-diaphragm gap width is about 250 microns. The circuit operates as follows:

The rf detector output is attenuated by the Nexus SQ10a amplifier in the overload protection circuit, as shown in Figure 4. When the output of the amplifier exceeds .6 volts, either positive or negative, one or the other 2N3646 transistors will be driven into conduction. The immediate effect is then to reduce the gate-voltage of the 2N2608 FET from 12 volts to about

.6 volts, so that the FET impedance is reduced to a few ohms. Since the cathodes of the 6CB5 pentodes are now essentially grounded by this FET, the plate current is sharply increased, and the electrode voltage drops. This serves as a stopgap, by immediately increasing the restoring force on the diaphragm. However, such heavy plate currents, would, if sustained, damage the tubes or the circuit. Therefore, a relay (K1 in Figure 4), which disconnects the high-voltage supply, is activated and latched by the sub-circuit incorporating the 2N2367 and 2N3640 transistors. Normally, these transistors are not conducting, but the drop in 2N3646 emitter voltage switches them on; they remain on, drawing current through the relay coil, until the reset switch is opened.

The 1N695 diode in this sub-circuit protects the transistors from possible damage by the voltage spike induced in the relay coil. It will be noted that both responses of the overload protection circuit, viz., grounding the high-voltage amplifier cathode and disconnecting the high-voltage supply, are necessary. Grounding the cathode provides immediate protection for the diaphragm and electrodes by stiffening the diaphragm, but the increased plate current, if sustained, would endanger the rest of the circuit. Activating the latching relay requires several milliseconds, but once accomplished, leaves the circuit entirely safe.

6. Voltage Ratio Control

The voltage ratio control circuit (see Figure 4) is a simple feedback circuit which fixes the ratio of the static voltages applied at the two electrodes,

independent of the size of these voltages, to any desired value. This is accomplished by sampling the electrode voltages with two high-impedance voltage dividers; the outputs of these dividers are compared by the Nexus SQ10a differential amplifier, which in turn feeds the right-hand control grid of the high-voltage amplifier. The capacitors in this circuit serve as audio filters. In this way, any drift of the electrode voltages relative to one another is prevented by an automatic adjustment of the control grid voltage. Furthermore, by a proper selection of the electrode voltage ratio, voltage-induced zero-shifts can be minimized, as previously discussed.

Experimental Details

Diaphragm Gauge

Figure 1 shows the significant dimensions and construction materials of the commercial diaphragm gauge* we have adapted for our tests. The general quality of the gauge, in terms of reproducibility, temperature stability, and electrode symmetry, are quite satisfactory. However, for our application, the gauge has a serious deficiency, viz., the surface strength and finish of the electrodes and, perhaps, the diaphragm as well, are inadequate at the field strengths employed. This is no discredit to the manufacturer; if used as intended, only rf fields on 10^2-10^3 volts/cm would be applied to these surfaces, whereas in our application, electrostatic fields of 10^4-10^5 volts/cm are applied as well. Each electrode consists of a 1000 Å layer of evaporated aluminum, overlaid with a 100 Å layer of TiO_2, on a quartz substrate; this aluminum layer has been gradually eroded away by high-voltage discharges. Indeed, the electrodes failed half way through the program and were returned to the manufacturer for recoating. A second failure occurred shortly before the completion date of the program. We shall discuss the high-voltage discharge mechanism, and its effects on our measurements, later in this section.

Vacuum System

Figure 7 is a schematic of the vacuum system employed in these tests. The cold-trap and pumps are standard,

* Model 110-CAP-0.05 D Differential Pressure Capsule Lion Research Corporation, Newton, Mass.

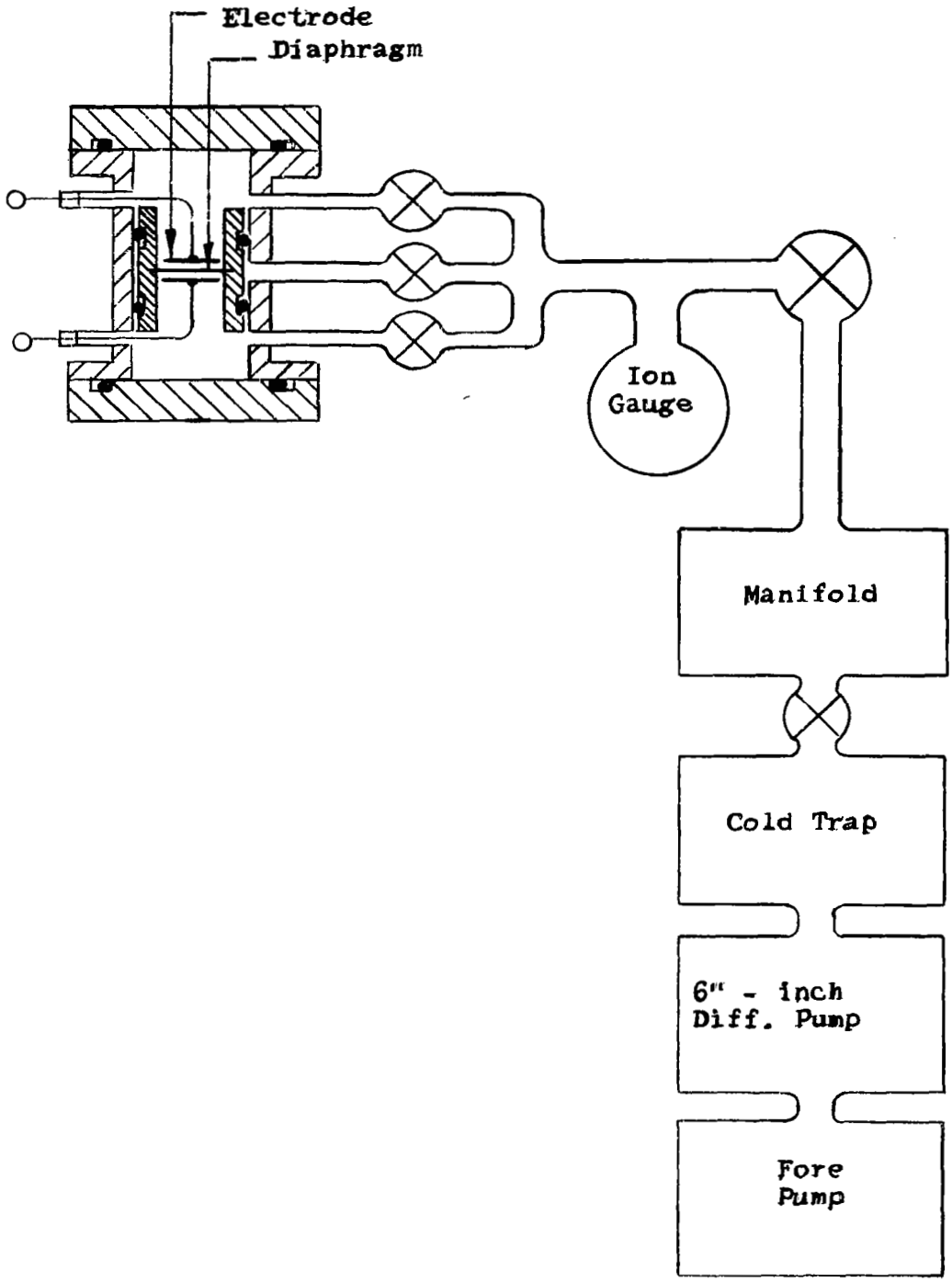

Figure 7 Schematic of Vacuum System

and require no comment. With the inlet valve to the manifold closed, the manifold pressure can be maintained at about 1×10^{-8} Torr, without baking. However, the ultimate pressure in the section containing the diaphragm gauge and NRC 563 ionization gauge was about 1×10^{-5} Torr, as measured with the ion gauge. This relatively poor vacuum is attributable to small leaks, discovered by helium leak testing, in the gaskets which seal the ion gauge and an adjacent spare port. The diaphragm gauge and its adjacent valves were leak-free; in fact, these valves could be closed for several minutes with no appreciable increase in diaphragm gauge pressure. Thus, the following test procedure could be employed:

Pressure was slowly built up on one side of the diaphragm, the opposite side being sealed off at a pressure of 10^{-5} Torr. The rf detector output (see preceding discussion of the electronic circuitry) was filtered to remove its audio component, and then fed to the Y-input of an X-Y recorder. The X-input was obtained from an NRC 763 ionization gauge control, fed by the NRC 563 ionization gauge. Figure 8 shows the results of two typical runs; one run with no voltage applied to the electrodes, and the other with 500 volts applied. In each run, the pressure was measured on one side of the diaphragm, and then, after evacuation, on the other. The pressure was built up simply by closing off the manifold inlet, and was presumably due to atmosphere leaking in at the gaskets referred to in the preceding paragraph. The time required to arrive at a pressure of 10^{-3} Torr was about 100 sec.

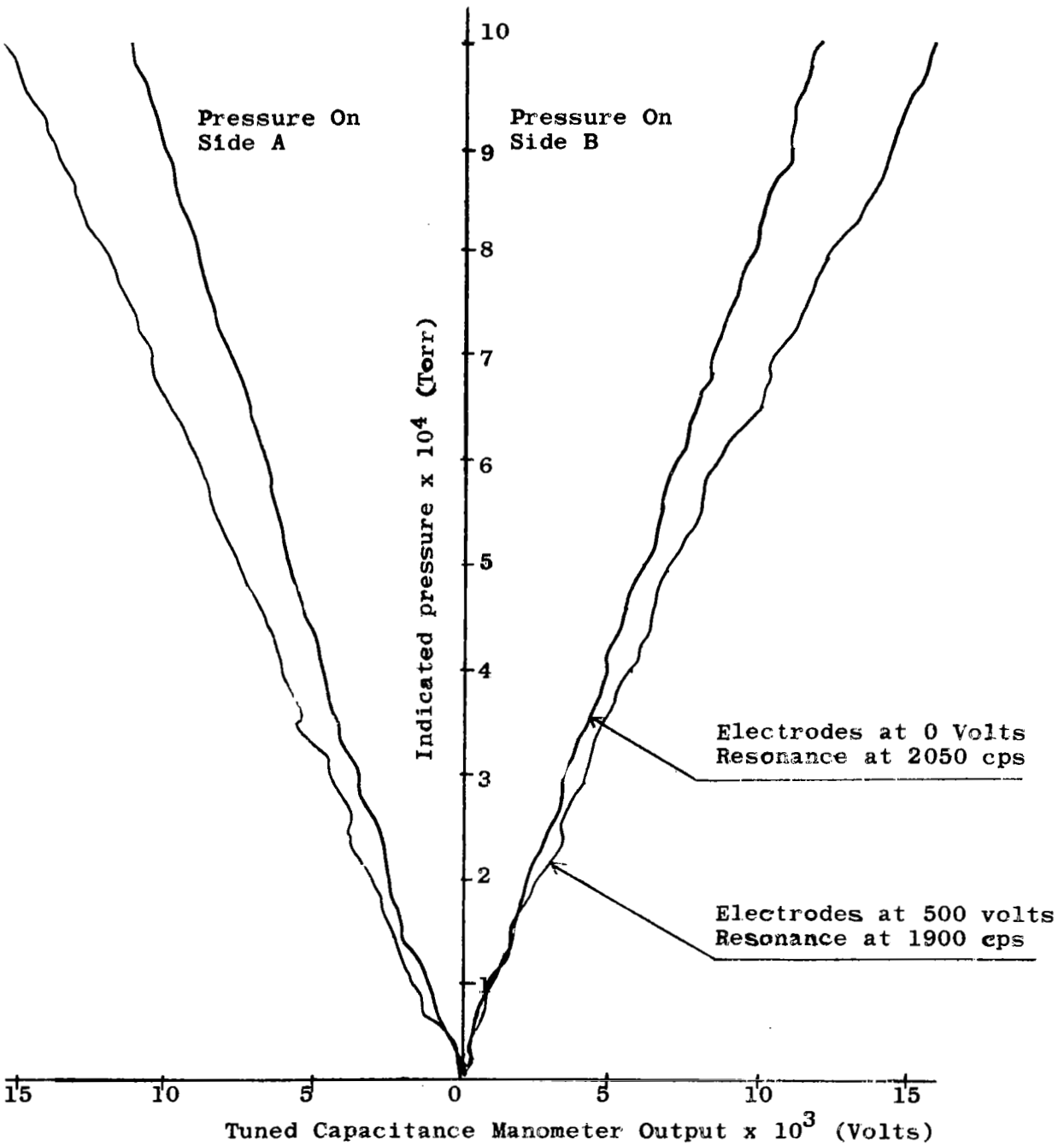

Figure 8

Gauge Output vs. Pressure

It can be seen that the uncertainty in these measurements is no greater than about 5×10^{-5} Torr, even when the gauge is being operated in the conventional manner with no electrostatic enhancement of its sensitivity. What is significant in these plots is that the electrostatic enhancement of the sensitivity does not introduce additional noise or instability. It should be emphasized that these measurements were made under relatively unfavorable conditions, that is, without temperature control, without a vibration-free mounting, and in particular, with the aluminized electrode surfaces suffering continual deterioration through high-voltage breakdown. This last condition is one which has prevented us from proceeding to higher voltages, where really large increases in sensitivity can be obtained, but should be readily correctible if a more suitable electrode material, say polished stainless steel, is employed.

One noteworthy feature of these plots is that the sensitivity increases with voltage at a much greater rate than was originally anticipated. If we plot the observed values of $\frac{dC}{dP}$ against V, and compare these with the theoretical prediction of Eq. (23), as shown in Figure 9, it is seen that agreement is poor at values of V near 600 volts. Although we have confidence in the theory, it is not easy to argue this discrepancy away as a correctible instrumental effect. When fixed capacitors were substituted for the diaphragm gauge, the output of the bridge circuit was found to be totally independent of the superimposed voltage V. Piezo-electric deformation of the quartz electrodes, polarization of the gas admitted to the gauge, ionic bombardment of the diaphragm, and other voltage-dependent phenomena have been considered, but all of these are orders of magnitude too small to account for

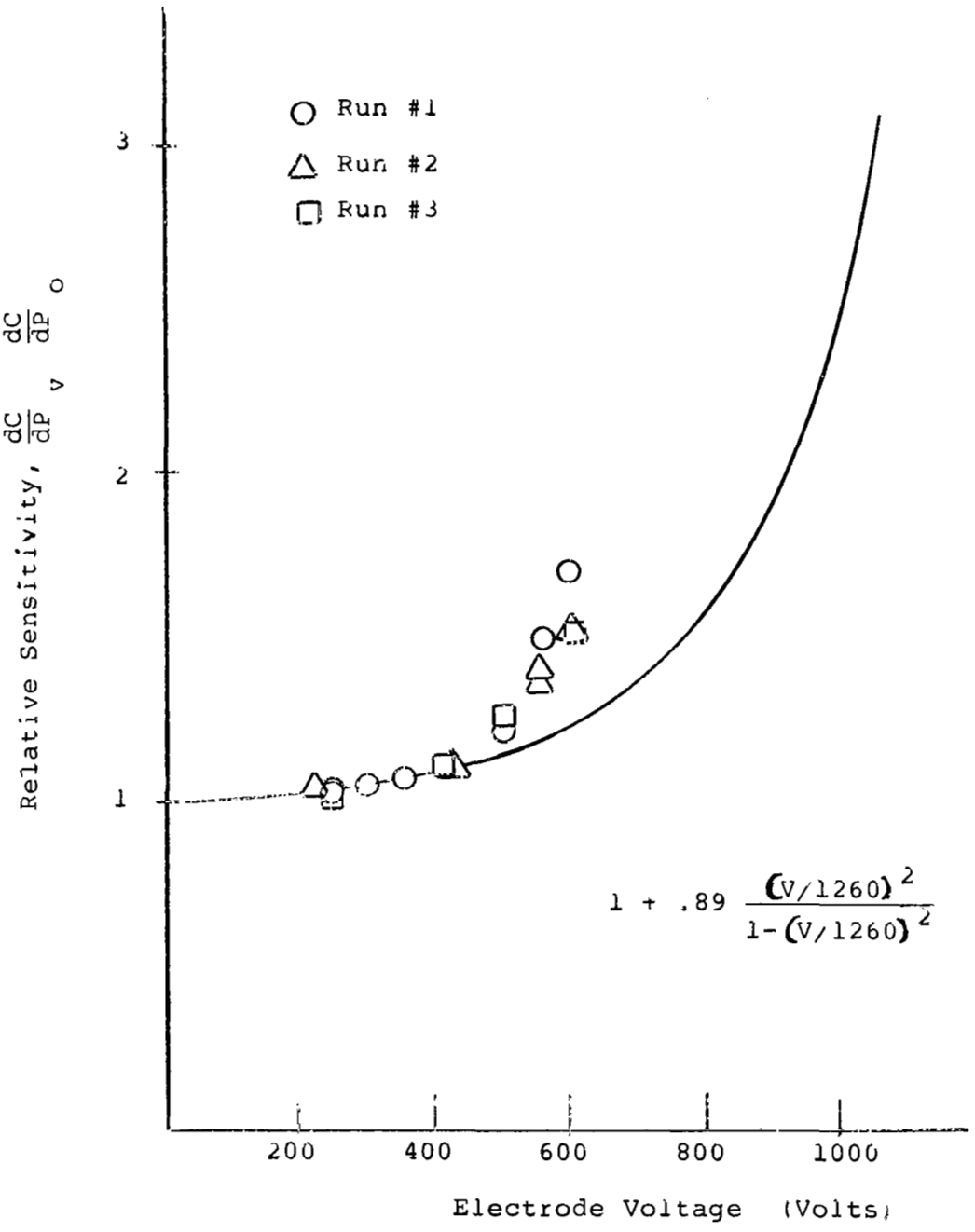

Figure 9

Normalized Gauge Sensitivity vs. Electrode Voltage

the discrepancy. One mechanism exists which seems at least plausible, but which unfortunately cannot now be quantitatively verified, the electrodes having failed again. This mechanism, which involves the breakdown at the electrode surface, arises as follows:

The erosion of the gauge electrodes has most probably been caused by high-voltage breakdown (vacuum breakdown); certainly, a pressure-independent breakdown of some kind has been found, through oscilloscopic observation, to occur in the electrode-diaphragm gap. This discharge was self-quenching and periodic, i.e., had the character of a relaxation oscillation, and had a threshhold of several hundred volts. What is significant to us is that both the charge transfer (10^{-6}-10^{-7} coulombs) and the repetition rate (0-100 cps) of the discharge were observed to depend strongly on the field strength in the electrode-diaphragm gap. In other words, as the diaphragm was displaced toward either electrode, the intensity and repetition rate of the discharge increased at that electrode and decreased at the other, even at a fixed voltage. Only rough measurements of this phenomena were made before the electrodes failed, but it is clear that such an effect could cause a spurious increase in signal, since the rf voltage at the low-impedance (high capacitance) electrode would be clipped more strongly and more often than at the high-impedance electrode. In fact, our estimate indicates that such spurious signals could result in a far larger error in sensitivity than the actual discrepancy for which we are trying to account; much depends on the time-profile of the discharge pulse, and on its exact dependence on field-strength. Merely as

speculation, we have considered possible causes for this periodic discharge, and it seems at least plausible to us that the discharge is initiated by field-emission at the diaphragm, and is quenched by free-electron charging of the TiO_2 layer which covers the aluminized quartz electrode. On this basis, the repetition rate of the discharge would in part be determined by the migration time of the free electrons across the TiO_2 layer. In any case, it is clear that such phenomena can be minimized in future designs by careful surface treatment of the electrodes and diaphragm, and also by choosing a plane-parallel electrode geometry so as to avoid field concentrations in the gap.

Prospects for Improved Performance

As discussed above, our experimental results have tended to confirm the theoretical evaluation of the electrostatically-tuned capacitance-manometer concept. The variation of resonant frequency with electrode voltage, and the general performance of the circuit, are as anticipated. To be sure, we are not wholly satisfied by our tentative explanation of the anamolous increase in gauge sensitivity near 600 volts. However, we are confident that the explanation does lie in the realm of instrumental effects, and that the anomoly can be eliminated by appropriate design changes. In considering the prospects for this gauge, we will then assume that our understanding of its operation is complete, and that certain obvious improvements will be incorporated in future designs. These improvements would include a vibration-free mounting, temperature-control, an appropriate choice of material and surface finish for the electrodes and diaphragm, and, of course, high-vacuum integrity and bakeability. Nevertheless, we shall see that in the present mode of gauge operation, there would be an uncertainty in pressure of at least 10^{-6} Torr. This uncertainty is associated with the possibility of changes occuring in work function, on admitting gas to the system. However, it will be further shown that such uncertainties can be eliminated if the electrode voltages are appropriately modulated.

Work Function

In the preceding theoretical treatment, it has been assumed that the electrostatic field in each gap is equal to the ratio of the applied voltage, V, to the gap width, d. This is inexact; the electrostatic field E is properly given by

$$E = \frac{V+\Phi_d-\Phi_e}{d} \tag{29}$$

where Φ_d and Φ_e are the work functions at the diaphragm and electrode surfaces respectively. Suppose now that the rest position of the diaphragm has been established with the gauge evacuated, but that on exposing one side of the diaphragm to gas, the quantity $\Phi_d-\Phi_e$ changes by an amount $\delta\Phi$. The measured pressure will then, unknown to the experimenter, be in error by an amount P_Φ, given by

$$P_\Phi = \frac{V\delta\Phi}{4\pi d^2} \qquad \text{dynes/cm}^2 \tag{30}$$

where d is in cm, and where V and Φ are in statvolts (1 statvolt = 300 volts). If we assume that even under the best conditions, changes in work function will be indeterminate to about 1 millivolt, Eq. (30) predicts an uncertainty in pressure of at least 10^{-6} Torr, given that V 1000 volts and d $\approx$ .25 mm.

To avoid this uncertainty, a sensible procedure would be to compare readings obtained at different voltages V. One should then, in principle, be able to

identify both P_ϕ and the true pressure P, since the former is proportional to V, while the latter is independent of V. In this regard, although far afield from our original purpose, we should note that the electrostatically-tuned capacitance-manometer could be used to measure work functions as readily as pressures. Be that as it may, we have now to consider what voltage modulation scheme should be most suitable.

Voltage Modulation

Let $\sigma(V)$ denote the sensitivity of the electrostatically-tuned capacitance-manometer, let P be the true differential pressure, and let $\delta\Phi$ be the uncertainty in work function. Then the output signal S(V) may be defined as

$$S(V) = \sigma(V) \left\{ P + \frac{V\delta\Phi}{4\pi d^2} + \alpha(V) \right\}, \tag{31}$$

where $\alpha(V)$ represents the residual dependence of rest-position on electrode voltage, to be expected if the effects of electrode asymmetry cannot be compensated at all voltages by a single setting of the voltage-ratio control. Suppose now that, in the present mode of operation of the gauge, we were to compare the values of S at two different voltages. The difference $S(V_1)-S(V_2)$ is given by

$$S(V_1)-S(V_2) = P\left(\sigma(V_1)-\sigma(V_2)\right) + \frac{\delta\Phi}{4\pi d^2}\left(V_1\sigma(V_1)-V_2\sigma(V_2)\right) + \alpha(V_1)\sigma(V_1)-\alpha(V_2)\sigma(V_2) \qquad (32)$$

Since $\sigma(V)$ increases with V, it is clear by inspection that the uncertainty in $S(V_1)-S(V_2)$ is greater than that of $S(V)$ alone. Indeed, in the low-voltage limit where $\sigma(V)$ is essentially constant, the difference signal $S(V_1)-S(V_2)$ is essentially independent of P. Perhaps, if one made enough measurements at different voltages, one could finally identify P. However, there is a far more direct way of eliminating the uncertainty; one need simply reverse the sign of V. It is physically obvious that both $\sigma(V)$ and $\alpha(V)$ depend only on the magnitude of V; hence, the quantity $S(V)+S(-V)$ will be independent of $\delta\Phi$, and furthermore, there will be no uncertainty in $\alpha(V)$, since the rest position of the diaphragm can be found with the gauge evacuated.

The necessary modifications of the circuitry would be straight-forward. The electrode voltages would be square-wave modulated at a frequency of, say, one-twentieth of the driving frequency; this square-wave voltage would swing alternately positive and negative with respect to the diaphragm potential. It is, in principle, immaterial whether the diaphragm is grounded, and the cathode potential of the pentode pair (see Figure 4) is several hundred volts negative, or whether the diaphragm is raised to a positive potential, and the pentode cathodes remain near ground. Either arrangements would have experimental advantages and disadvantages which

we will not attempt to weigh here. The important consideration is that the feedback incorporated in the phase detector circuit should reverse in sign along with the electrode voltage; otherwise, the diaphragm would be driven away from the resonance on the "wrong" half-cycle. In addition, it will probably be necessary to vary the audio oscillator frequency so as to keep the diaphragm at resonance throughout the transition from positive to negative electrode voltage.

In this experimental arrangement, the rf detector output would be composed of a steady term proportional to the true pressure differential P, an alternating term, proportional in amplitude and synchronous in phase with the diaphragm vibration, and another alternating term, at the square-wave frequency, proportional to any difference in work function, $\delta\Phi=(\Phi_d-\Phi_e)_a-(\Phi_d-\Phi_e)_b$, where Φ_d and Φ_e are the work functions of diaphragm and electrode respectively, and where a and b refer to the two sides of the diaphragm. It should be noted that if Φ_d and Φ_e are unequal, the action of the phase detector, in bringing the diaphragm to resonance, will result in unequal positive and negative swings of electrode voltage with respect to the diaphragm (see Eq. (29). This will not introduce error, except insofar as $\alpha(V)$ may be affected, but it would probably be advisable to construct the diaphragm and electrodes of the same material. Doing so would in any case diminish $\delta\Phi$. With these modifications, it should be possible with careful technique to employ the electrostatically-tuned capacitance-manometer at pressures well below 10^{-6} Torr.

SUPERCONDUCTOR BOLOMETER GAUGE

General

In our preliminary discussion of the limits of absolute pressure measurements, we had concluded that the measurement of energy flux from a velocity-modulated source, or from a source moving at fixed velocity relative to the detector, could under certain conditions serve as the basis for the absolute measurement of pressure. These conditions are that inter-molecular collisions occur far less often than collisions with the source or detector, and that the nature of the molecular energy exchange at both source and detector be known. This second condition is by no means easy to fulfill, since the degree of thermal accomodation will vary with gas composition, surface condition, and temperature. It will be seen, however, that the experimental arrangement we propose satisfies this requirement for a large number of gases.

Assuming the above conditions to be fulfilled, the measurement of absolute pressure will be limited by the sensitivity or by the signal-to-noise ratio of the detector. This is in contrast to the case where it is the momentum flux from a temperature-modulated source that is measured, so that radiation-pressure contributes to the signal. In the present case, the radiant energy background would contribute to the noise, but not the signal, since the source velocity will assuredly be sub-relativistic.

Turning now to the problem of measuring the energy flux from a velocity-modulated source, we note first that bolometers are the most sensitive thermal-energy

detectors known. A bolometer is a film whose electrical resistance is strongly temperature-dependent, when operated at temperatures in the liquid helium range, such films have been used to detect infrared radiation at levels as low as 10^{-10} watts/cm^2, with characteristic response times of the order of 1 sec. We shall base our discussion of the sensitivity and noise level of bolometers on the treatment given by Newhouse.[1]

Bolometer Sensitivity

Consider a bolometer film, one surface of which is exposed to molecules arriving from a velocity-modulated source. For the moment, we will ignore the steady component of this flux, for this component only affects the operating point and noise level of the bolometer. We just wish to consider the variations in bolometer temperature induced by the alternating component Q_v of the energy flux, and to relate the variations in bolometer resistance to these temperature variations.

We will suppose that the bolometer has a heat capacity C per unit area, and that it is weakly coupled, by a poor thermal conductor, to a heat sink at temperature T_o. Additional heat transfer will occur through radiation, and possibly through the evaporation of gas molecules. The bolometer temperature will be expressed as $T=T_o+\tau$, where τ is the response to Q_v; at the very low pressures we hope to measure, it may safely be assumed that $\tau<<T_o$. It should be realized that we are ignoring whatever steady temperature difference exists between the bolometer and the heat sink, but this difference will be kept small in the actual experiment.

It will be useful in approaching this problem to examine an analogous electrical circuit, shown in Fig. (10a). The alternating component of energy flux, Q_v, will be treated as a current I, while the temperature response will be treated as a voltage V. Each of the mechanisms for bolometer heat loss will be treated as a thermal resistance, viz., conduction to the heat sink is denoted by R_{cond}, radiation is denoted by R_{rad}, and evaporation, should it occur, is denoted by R_{gas}. Joule heating of the bolometer by the electrical current used in measuring its resistance will be treated separately.

From Eq. (6) and Eq. (2) we have

$$I = Q_v = 3.75 \times 10^{-8} pv \cos \omega t \quad (\text{watts/cm}^2) \tag{33}$$

$$R_{rad} = \frac{1}{2}(4\sigma\varepsilon_o T_o^3)^{-1} \quad (^oK\text{-cm}^2/\text{watt}) \tag{34}$$

$$R_{gas} = 1.6 \times 10^8 T_o/9p\bar{v} \quad (^oK\text{-cm}^2/\text{watt}) \tag{35}$$

where p is expressed in dynes/cm^2 (equivalently, in μbar), where the source velocity amplitude v and the mean evaporation velocity $\bar{V}$ are expressed in cm/sec, where ε_o is the bolometer emissivity, and where a factor 1/2 has been included in the expression for R_{rad} to account for radiation from both film surfaces. It will be noted that for those gases which are cryosorbed at the bolometer surface, R_{gas} should be taken to be infinite; indeed, Eq. (35) will be appropriate for only one gas, helium, if the bolometer is near 4.2°K.

As for R_{cond}, it will be necessary to provide sufficient conductance to the heat sink to accomodate the steady heat input from the source, principally radiation. As good practice, the bolometer temperature should be kept fairly close to the heat sink temperature T_o, say at a temperature of $1.1T_o$. Therefore, it will be necessary that

$$R_{cond} \lesssim .1T_o(\sigma\varepsilon_o T_s)^{-1} \qquad (^oK\text{-}cm^2/watt) \tag{36}$$

where T_s is the source temperature.

Let us now consider a definite experimental configuration. The bolometer will be a superconducting film, held at a temperature, say of 4.2^oK, which is within the resistive transition region of the film. The gas will be condensable, so that R_{gas} can be ignored. The source will be well above 4.2^oK, so that R_{rad} can be ignored by comparison with R_{cond} (compare Eq. (34) with Eq. (36). However, the equivalent circuit for the modulated component of energy flow is not simply given by R_{cond} in parallel with C. We must further ask what effects an impressed electrical current will have on the heat balance of the film. If, as is usually the case, the bolometer is incorporated in a Wheatstone bridge whose fixed arms have a much higher resistance than than of the bolometer, the electrical current i through the bolometer will be constant. Hence, the Joule heating of the bolometer, $Q_J = i^2R$, increases in direct proportion to its electrical resistance R. Now $R=R_o+\tau\frac{dR}{dT}$, so that

an increase in Joule heating accompanies any increase in the energy flux Q_v. Thus, the temperature response t will be enhanced by this favorable contribution of Joule heat. The bolometer response is as if R_{cond} had been increased to a value R'_{cond}, given by

$$R'_{cond} = \frac{R_{cond}}{1-i^2\frac{dR}{dT}R_{cond}} \tag{37}$$

It might be asked why the above considerations do not apply equally in estimating, as in Eq. (36), the value of R_{cond} needed to maintain the bolometer temperature close to that of the heat sink. The point is that $\frac{dR}{dT} >> \frac{R_o}{T}$ for superconductors in the resistive transition region, so that the steady Joule heat input, i^2R_o, can be neglected by comparison with the radiant energy flux from the source.

The equivalent circuit for the alternating component of energy flow to the bolometer is then given by R'_{cond} in parallel with C, as shown in Figure 10b. We will suppose that the combined thickness of the bolometer and whatever substrate supports it is perhaps 10^{-3}cm, so that $C \simeq 10^{-6}$ watt-sec/cm^2-^oK. It seems reasonable to take $R'_{cond} \simeq 10\ R_{cond}$; at larger values of R'_{cond}, instabilities should be expected. Now it is clear by inspection of Figure 10b that the maximum amplitude of the temperature response will be obtained if $\omega CR'_{cond} \simeq 1$. However, for $T_s = 77^oK$, it can be seen from Eq. (36) and the assumed value of C that $CR'_{cond} \simeq$ 1 sec., so that one is really restricted to essentially

dc operation of the bolometer. On this basis, we have

$$\tau = Q_v R'_{cond} \simeq \frac{3.75 \times 10^{-8} pvT_o \cos \omega t}{\sigma \varepsilon_o T_s^4} \qquad (38)$$

Substituting $T_o = 4.2^oK$ and $T_s = 300^oK$, assuming the bolometer to be polished to the extent that $\varepsilon_o \simeq .03$, and further assuming that a steady source velocity, v, of 1000 cm/sec can be attained, we find that $\tau \simeq .1^oK/\mu$-bar. If the source temperature were 77^oK rather than 300^oK, we would have $\tau \simeq 20^oK/\mu$-bar.

On the basis of the experiments reported by Martin and Bloor[2], we will assume that the minimum detectable change in bolometer temperature is about $10^{-5o}K$. It then follows from the preceding paragraph that, for a source whose velocity is 1000 cm/sec and whose temperature is 300^oK, the minimum detectable pressure will be 2×10^{-7} Torr; if the source is cooled to liquid nitrogen temperature, the minimum detectable pressure will be about 5×10^{-9} Torr.

Noise

It should certainly be asked whether the minimum detectable change in bolometer temperature is, in this experimental arrangement, above the thermal noise background. By far the largest contribution to the bolometer noise is made by radiation from the source. The mean-square value $\overline{P_n^2}$ of the noise-power received from the source is given by

$$\overline{P_n^2} = 8\sigma\varepsilon_o kT_s^5 \Delta f \qquad (39)$$

where $k=1.38 \times 10^{-23}$ watt-sec/^oK is Boltzmann's constant, and where Δf is the bandwidth. Then, assuming that $\Delta f \approx 1$cps and that $\varepsilon_o \approx .03$, we have $P_n \approx 10^{-11}$ watts at 300^oK, and $P_n \approx 5 \times 10^{-13}$ watts at 77^oK. In both cases, P_n is far below the molecular energy flux from the moving source at the respective minimum pressures of 2×10^{-7} Torr and 5×10^{-9} Torr (see Eq. 32). Thus, such pressures can be measured by a bolometer, and indeed, still lower pressures, if the present bolometer temperature sensitivity can be increased.

Experimental Arrangement

Figure 10c is a schematic of a possible bolometer gauge configuration. Two bolometers are employed in a balanced arrangement, the energy flux to one bolometer being increased, and that to the other being decreased, by the steady rotation of the cylinder. The cylinder, and the guard wall around the bolometers, would be maintained at a temperature of 77^oK. This would permit the study of a respectable number of gases but would not place as severe a heat load on the bolometers as would be the case if the cylinders were at 300^oK. A significant advantage of the balanced arrangement of the bolometers is that variations in cylinder temperature will affect both bolometers equally. Furthermore, the bolometers can be balanced, with the cylinder rotating, by simply moving them to the cylinder

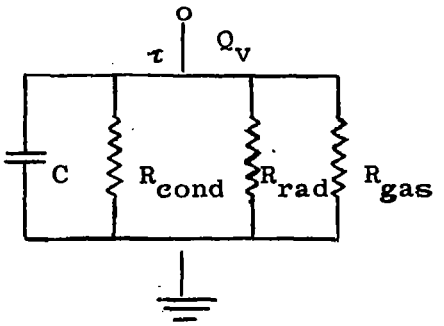

(a) Thermal circuit of Bolometer.

(b) Bolometer well-anchored to Heat-Sink, and carrying electrical current i .

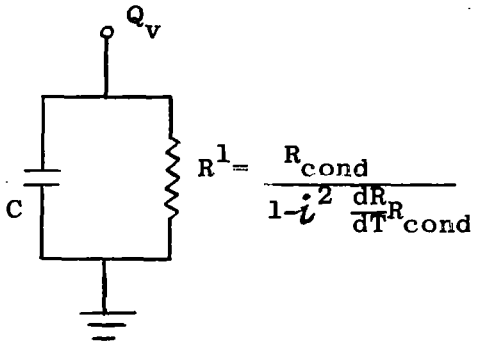

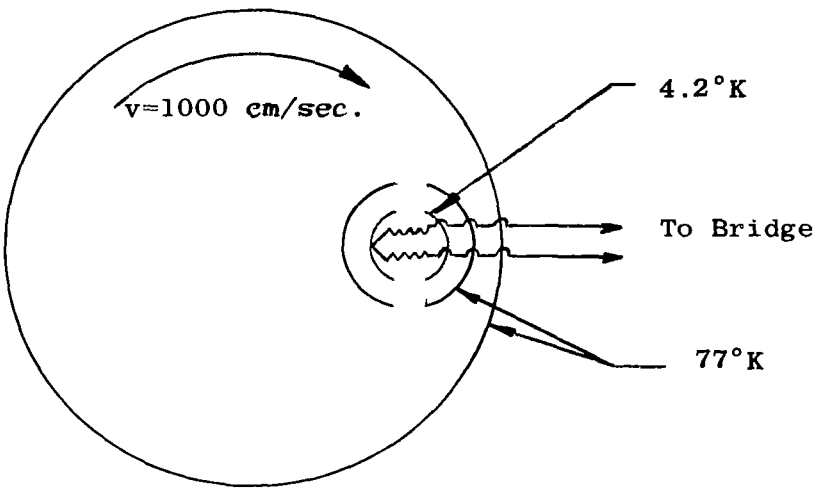

Figure 10 Schematic of Superconducting Bolometer Gauge

axis. The operating point (average temperature) of the bolometers can be stabilized by feedback adjustment of the bridge current. Such a bolometer gauge would theoretically permit absolute pressure measurements at about 5×10^{-9} Torr.

Molecular Beam Detector

Since the apparatus described above includes rotating components and a fairly intricate cryogenic system, all inside a UHV system, it might be desirable to consider less complex applications of the superconducting-bolometer detection concept. A bolometer could simply be installed in a conventional UHV molecular beam calibrator; there would be no moving parts and the main chambers of such calibrators are in any event operated near $4.2^{\circ}K$. Furthermore, the molecular energy flux incident on the bolometer would be roughly $\frac{1}{2}mv^3n$, where n and v are the beam density and velocity respectively. With the reported sensitivity of bolometers being about 10^{-10} watt/cm^2, and assuming a furnace temperature of $300^{\circ}K$, it follows that beam densities of about 10^6 per cc can be detected. Thus, in a molecular beam calibrator, a bolometer would be about as good a detector as a nude ionization gauge, and would be absolute as well. Again, two bolometers could be employed in a balanced arrangement, one facing toward the beam and one facing away. If necessary, the beam could be chopped by a simple mechanical shutter; this could be magnetically operated to avoid complicated mechanical linkages. Finally, sticking probabilities of low boiling point gases such as hydrogen or neon could be measured with bolometers; the detected energy flux would decrease in direct proportion to the sticking probability.

MODULATED GAS-TEMPERATURE GAUGE

In the discussion of the limits of absolute pressure measurement, it was noted that the measurement of momentum flux from a temperature-modulated source could, under certain conditions, serve as the basis for an absolute measurement of pressure. These conditions are that inter-molecular collisions occur far less often than collisions at the source and detector surfaces, that there be full thermal accomodation of molecules striking the source or detector surfaces, and that thermal radiation contribute negligibly to the momentum flux. It was further noted that as the modulation frequency decreases, both the sensitivity of the detector and the magnitude of the temperature variations (for fixed source power) also increase. It is then clear that the maximum sensitivity can be obtained by operating with a fixed temperature difference between source and detector, as in the Knudsen gauge. However, there are certain experimental advantages to operating at a low audio frequency; in particular, amplifiers can be tuned to the modulation frequency. We shall consider two general methods, direct heating and thermoelectric heating, for modulating source temperatures, and further consider what pressures could then be detected with existing microphones.

Modulation of Source Temperature

As one possibility for direct modulation of the source temperature, we will suppose the source to be a

thin metal film on a transparent substrate of low thermal conductivity. Behind the substrate is an infra-red lamp, whose output is chopped by, say, a rotating shutter. Thus, bursts of infra-red radiation are beamed through the substrate, but are absorbed by the metal film. Alternatively, the film could be heated resistively, simply by passing an alternating current through it. The substrate would again be required to have low thermal conductivity, but need not be transparent.

The heat flux q to the film can be expressed as $q=q_o\ (1+\cos\ \omega t)$, and if we assume that the rear surface of the substrate is anchored to a heat sink, the temperature difference ΔT between the film and the heat sink is readily found to be

$$\Delta T = \frac{q_o}{K}\left[L + \sqrt{\frac{K}{\omega C}}\ \cos\left(\omega t+\frac{\pi}{4}\right)\right] \qquad (40)$$

where K is the thermal conductivity of the substrate, where L is the thickness of the substrate, where $\frac{\omega}{2\pi}$ is the chopping frequency, where C is the volume heat capacity of the substrate, and where it is assumed that $L>>\sqrt{K/\omega C}$. Before discussing what values these quantities might have, an alternative method of modulating the source temperature, thermoelectric heating, will be considered.

We will now suppose the source to be an array of thermocouple junctions, i.e., a thermopile. Let the current density J in the individual thermocouples be given by $J=J_o \cos \omega t$, and let the average thermo-electric power and electrical resistivity of the individual

thermocouples be Q and ρ respectively. Then assuming that the thermocouple junctions are packed closely enough to approximate a plane, the temperature response ΔT of this plane with respect to the rear junctions of the thermopile will be given by

$$\Delta T = \frac{J_o^2 \rho L}{2K} \left\{ \frac{L}{2} + \frac{QT}{J_o \rho L} \sqrt{K/\omega C} \cos\left(\omega t + \frac{\pi}{4}\right) \right\} \qquad (41)$$

where K is the thermal conductivity of the thermo-electric material, where T is the absolute temperature, where L is the length of the thermocouples, and where it is again assumed that $L \gg \sqrt{K/\omega C}$.

Now comparing Eq. (40) and Eq. (41), we see that the coefficient q_o in Eq. (40) and the coefficient $J_o^2 \rho L/2$ in Eq. (41) are the respective power inputs per unit area of the source. Thus, assuming K and C to be comparable for the transparent substrate in the first case, and the thermocouple material in the other, it is clear that the comparative efficiency of these methods of temperature modulation will depend on the size of the quantity $2QT/J_o \rho L$. The most suitable thermocouple material would probably be Bi_2Te_3 for which $QT \approx 60$ millivolts near 300^oK, and for which $\rho \approx 5 \times 10^{-4}$ Ω-cm. It follows that a thermoelectric source will be inferior to the directly heated source unless $J_o L$ is less than 200 amps/cm. Now L cannot be made indefinitely small; a reasonable value for L would be 1 cm. Therefore, the thermoelectric method will be inferior unless the power input $J_o \rho L/2$ is less than 10 watt-sec/^oK-cm^3, and $\omega \approx 100$, we see from Eq. (41) that a 10 watt/cm^2

input power would produce an alternating temperature amplitude of only .3°K. Therefore, direct heating must be the preferable method of the two choices.

Taking the same values of $\omega \approx 100$ and $C \approx 1$ watt-sec/°K-cm^3 for the substrate as for the thermocouple, and assuming that K can be reduced to about 10 milliwatt-sec/°K-cm by lamination, we find that an alternating temperature amplitude of about 1°K/watt-cm^2 can be achieved with this method. If the laminated substrate is 1 mm thick (we recall that it is necessary that $L >> \sqrt{K/\omega C}$), the steady temperature drop across the substrate will be 10°K/watt. Now even for a substrate conductivity of 10 milliwatt-sec/°K-cm, radiant losses from the film would exceed the losses through the substrate at temperatures above 200°K. Therefore, the rear surface of the substrate would have to be cooled well below 200°K, say to 77°K, for the method to have any chance of success. Cooling would have the further advantages of reducing the heat capacity of the substrate, leading to a larger amplitude of the alternating temperature, and of increasing the ratio τ/T_s, by reducing T_s (see Eq. 3).

Based on the preceding discussion, a suitable experimental configuration is suggested schematically, in Fig. 11. It is clearly necessary to monitor the source temperature; for this reason, the exposed surface of the source will be a temperature-sensitive resistive film which will serve as a thermometer. An underlying resistive film will serve as a heater, and an insulating film between heater and thermometer will provide elec-

trical isolation. These films will be deposited on a substrate of low thermal conductivity, whose rear surface is cooled by a liquid nitrogen bath. A suitable substrate material would be fused quartz or pyrex, about 5 mm thick. On the basis of Eq. (40) above, we might then expect as typical operating conditions:

Mean source temperature.....150^{o}K
Frequency.....30 cps
Peak-to-peak temperature modulation.....30^{o}K
Power input.....1 watt/cm^{2}

From Eq. (3), the pressure in the neighborhood of the source would have a peak-to-peak modulation of about 20% of the absolute pressure. The pressure sensitivity of the gauge will then depend on the sensitivity of the detector, i.e., the microphone sensitivity. A conventional high-sensitivity condensor microphone will provide a signal of about 3 mv per μ bar (dynamic pressure), and we may reasonably assume that signals of 1μv, corresponding to dynamic pressures of 2.5×10^{-7} Torr, will be detectable.* In the example given above, the dynamic

* An existing gauge, the "sonic gauge", employs such a microphone to detect velocity modulation impressed on the gas by a mechanical transmitter. However, we have seen from Eq. (6) that such a gauge cannot be absolute. Furthermore, the operation of the gauge is limited by mechanical coupling between the transmitter and the microphone.

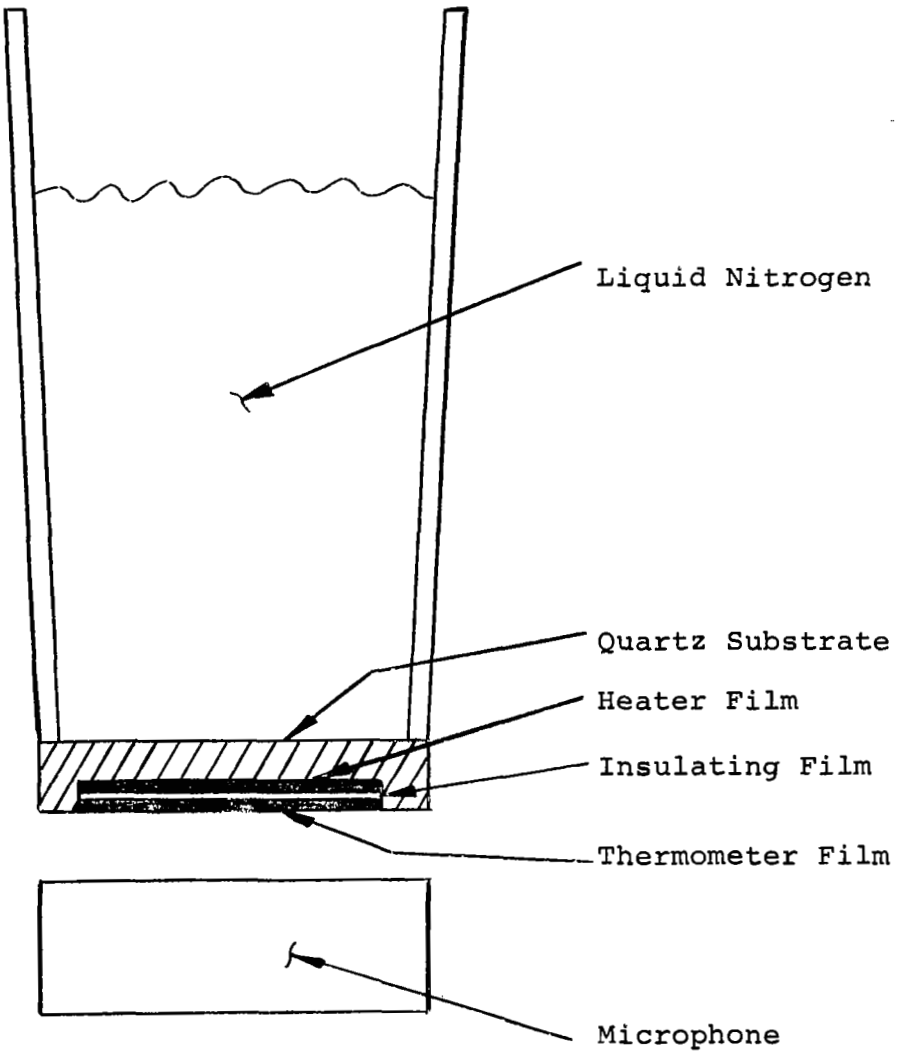

Figure 11 Schematic of Modulated Gas-Temperature Gauge

pressure is about one-tenth of the absolute pressure, so that absolute pressures of about 2.5×10^{-6} Torr would be detectable. Furthermore, conventional microphones have a higher frequency response than would be needed in this application; a special-purpose low-frequency microphone would doubtless serve to extend the range of the "modulated gas-temperature" gauge to pressure below 10^{-6} Torr.

CONCLUDING REMARKS

A theoretical and experimental evaluation of the concept of electrostatic control of capacitance-manometer sensitivity has been carried out. The results have been encouraging, although problems have been created by high-voltage breakdown at the electrode and diaphragm surfaces of the gauge. This breakdown can undoubtedly be eliminated by choosing more appropriate surface materials. It is hoped that absolute pressures well below 10^{-6} Torr can ultimately be measured with this gauge if uncertainties in work-function can be avoided; a voltage-modulation technique is suggested which should accomplish this.

It is suggested that the use of superconducting-bolometers to detect the kinetic energy of incident gas molecules will permit absolute measurements of pressures as low as 5×10^{-9} Torr, and also measurements of molecular beam densities as low as 10^{6} molecules/cc.

It is suggested that the juxtaposition of a low-frequency heater and a sensitive microphone will permit absolute pressure measurements as low as 10^{-6} Torr.

REFERENCES

1. Vernon L. Newhouse, Applied Superconductivity, (John Wiley & Sons, 1965) p. 248 ff.

2. Martin, D. H. and Bloor, D., Cryogenics 1, 159 (1961)